Geothermics 117 (2024) 102866

Contents lists available at ScienceDirect

Geothermics

journal homepage: www.elsevier.com/locate/geothermics

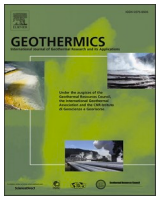

Regional- to district-scale controls on thermal springs occurrence in South Africa: Insights from investigations of their spatial distribution and their spatial relationships with geological features

Emmanuel John M. Carranza [a,b,*], Reinnie Ntokozo Maseko [b,c]

[a] Department of Geology, University of the Free State, Bloemfontein, South Africa
[b] Discipline of Geosciences, University of KwaZulu-Natal, Durban, South Africa
[c] Geovicon Environmental (Pty) Ltd, Middelburg, South Africa

ARTICLE INFO

Keywords:
Thermal springs
Low enthalpy
Geothermal
Spatial analysis
Geological controls

ABSTRACT

In the study presented here, the spatial distribution of thermal springs in South Africa was investigated using point distribution analysis, fractal analysis and Fry analysis, and the thermal springs' spatial relationships with high-heat-producing granitoids (HHPGs), groundwater yield, and structural lineaments were investigated using distance distribution analysis. The purpose of these spatial investigations was to explore the regional- to district-scale geological controls on thermal springs occurrence in South Africa. The results show that regional- to district-scale geological controls on thermal springs occurrence in South Africa involve the presence of or proximity to HHPGs (as heat source control), groundwater yield of ~2 L/s (as water source control) and intersections of structural lineaments with particular trends (as pathways control). In southern and eastern South Africa, the pathways controls are, respectively, intersections of ENE-trending lineaments with NNW- and NW-trending lineaments and intersections of ENE- and WNW-trending lineaments. This spatial information comprises a conceptual model that can be used as a framework for regional- to district-scale predictive modeling and mapping of the prospectivity (or likelihood) of areas where geothermal resources potentially exist in South Africa.

1. Introduction

Occurrences of hot or thermal springs are evidence of the presence of geothermal energy resource in the subsurface. The spatial distribution of thermal springs can be considered non-random because (a) their existence are known to be governed by an interaction between particular geological features or processes and (b) they are spatially related only with specific geological features. Thus, investigation of the thermal springs' spatial distribution of would be useful in deducing which geological features plausibly governed the existence of the former at their present locations. Besides that, investigation of the spatial relationships of thermal springs with specific types of relevant geological features would be useful in evaluating the relative import of the former as controls on occurrence of the former. These complementary spatial investigations would thus be instructive for conceptual modeling of geological controls on thermal springs occurrence at a specific spatial scale, which can be used as framework for predictive modeling of prospectivity for geothermal energy resource at the same spatial scale.

On regional-scale maps, locations of thermal springs are customarily shown as points. Describing the spatial distribution of point objects of a particular kind is achievable via point distribution analysis (Boots and Getis, 1988), fractal analysis (Mandelbrot, 1982) and Fry analysis (Fry, 1979). These three spatial analytical methods have been demonstrated by Carranza (2009) to deduce controls on mineralization associated with a geothermal system. Therefore, these three spatial analytical methods are likewise suitable for deducing controls on thermal springs occurrence, which is invariably associated with a geothermal system. Fry analysis has been applied by Carranza et al. (2008), Moghaddam et al. (2013, 2014) and Sang et al. (2017) to describe the regional-scale spatial distributions of thermal springs in West Java (Indonesia), in Iwate and Akita provinces (Japan) and in Liaoning province (China), respectively, to support analysis of prospectivity for geothermal resources. However, to the best of the authors' knowledge, based on review of relevant literature, point distribution analysis and fractal analysis have not been

* Corresponding author at: Department of Geology, University of the Free State, Bloemfontein, South Africa.
E-mail address: ejmcarranza@gmail.com (E.J.M. Carranza).

https://doi.org/10.1016/j.geothermics.2023.102866
Received 27 February 2023; Received in revised form 25 September 2023; Accepted 5 November 2023
Available online 16 November 2023

used yet to deduce geological controls on thermal springs occurrence.

As thermal springs and other types of geothermal sites are commonly structurally-controlled (e.g., Bell and Ramelli, 2009; Taillefer et al., 2018), recognizable orientations in the thermal springs' spatial distribution are typically attributed to controls by linear geological features (e.g., faults). However, there are certainly other non-linear geological features that control the occurrence of geothermal sites including hot springs; for example, igneous intrusions and radiogenic element-rich rocks, which are non-linear geological features although they may exhibit linear trends due to underlying tectonic controls, are typical heat sources of thermal springs and other types of geothermal sites (Basantaray & Mandal, 2022). Thus, for ample deduction of geological controls on thermal springs occurrence, an investigation of the spatial distribution of thermal springs should be complemented with an investigation of the spatial relationships of thermal springs with specific types of relevant geological features. The methods of spatial analysis that have been used to investigate the regional-scale spatial relationships of thermal springs with specific relevant geological features include spatial frequency distribution analysis (Carranza et al., 2008), distance distribution analysis (Carranza, 2009; Moghaddam et al., 2013), weights-of-evidence modeling (Zehner et al., 2006; Moghaddam et al., 2013; Sang et al., 2017), and data-driven evidential belief modeling (Carranza et al., 2008; Moghaddam et al., 2013).

In this paper, the above-proposed spatial investigations were conducted to explore the geological controls on thermal springs' occurrence on a regional-scale in South Africa. This research objective is based on the hypothesis that the spatial distribution of thermal springs is a function of geological controls. As novelty of the research described here, point distribution and fractal analyses were used besides Fry analysis to unravel the thermal springs' regional- to district-scale spatial distribution in South Africa, which would offer insight to controls by specific linear geological features. The main advantages of these spatial investigations are their graphical yet quantitative nature and, thus, the empirical nature of the results. However, instead of using all the four above-mentioned spatial analytical methods to investigate the regional-scale spatial relationships of thermal springs with specific relevant geological features, only distance distribution analysis was used here. That is because the mathematical formulations of each of the three other methods (i.e., analysis of spatial frequency distribution, modeling of weights-of-evidence, data-driven modeling of evidential belief) are akin to that of the distance distribution analysis, and Carranza (2002, 2008) has shown that all these four methods yield strongly similar results when applied to investigate the spatial relationships of hydrothermal mineral deposits of a specific type with geological features of certain types. The work presented here to deduce the regional- to district-scale geological controls on thermal springs occurrence in South Africa made use of publicly available relevant geoscience spatial data.

2. Thermal springs in South Africa

The mainland of South Africa, measuring 1,221,037 km^2, is situated on a stable continent and passive margin with no recorded recent volcanic activities (Kent, 1949; Tshibalo et al., 2015; Dhansay et al., 2017); but, it is characterized by a variety of complex geological settings. No summary account of South Africa's regional geology is given here because it has been described extensively in the literature (cf. Du Toit, 1954; Johnson, 1976; Fripp et al., 1980; Compston and Kröner, 1988; Thomas, 1989; Thomas et al., 1992; Van Reenen et al., 1992; Eriksson et al., 1995; Nowicki et al., 1995; Robb and Meyer, 1995; Johnson et al., 1996; Barnett et al., 1997; Schmitz et al., 2004; Catuneanu et al., 2005; McCarthy and Rubidge, 2005; Johnson et al., 2006; McCarthy et al., 2006).

Despite the lack of volcanic activities in the Recent past, 64 thermal springs occurrences have been documented in South Africa (Kent, 1949; Dhansay et al., 2017). The thermal springs' average temperature is $<$ 100 °C, namely 39.4 °C, indicating the likelihood of low-enthalpy geothermal resources in South Africa (Dhansay et al., 2017). Most of these thermal springs emerge along fissures, faults, contacts and dike intrusions (Kent, 1949), and in regions with high uranium concentrations (Dhansay et al., 2017) and high thorium and potassium concentrations as well (Madi et al., 2014). Inspection of the map in Fig. 1 indicates that 17 thermal springs exist on the Kaapvaal Craton, 14 on Limpopo Belt, 12 on the Cape Fold Belt, 11 on the Namaqua-Natal Belt, 9 on the Bushveld Complex, and 1 on the Witwatersrand Basin.

According to Dhansay et al. (2017), the South African regions that show high heat signatures of 60 mW/m^2 are mostly associated with granitoid rocks and/or orogenic belts such as the Cape fold belt, Namaqua-Natal belt and Limpopo belt, which surround the Kaapvaal Craton. In these regions, the likely source of heat for the thermal springs are concentrations of radiogenic U in the rocks. Dhansay et al. (2017) have shown that the Cape Granite Suite, Namaqua-Natal belt, Archean granites-gneiss, and felsic rocks of the Bushveld Complex have U concentrations of approximately 34, 10–54, 20–28 and 30 ppm, respectively. Rocks of the Transvaal and Witwatersrand Supergroups including rocks of the Pongola basins also show relatively high concentrations of uranium; hence, the high heat signatures in these regions (Dhansay et al., 2017). All these regions are endowed with thermal springs and have relatively higher groundwater level compared to the other parts of the country.

3. Methods of spatial investigation

3.1. Datasets/maps used

The thermal springs database of Dhansay et al. (2017) was used in this study. This database contains the 64 thermal springs' locations (i.e., longitude and latitude coordinates; Fig. 1), depth, temperature, estimated geothermal gradient, method of geothermal gradient calculation, and data sources. According to this database, the thermal springs' temperatures range from 26 °C to 67 °C with average of 39.4 °C and standard deviation of 57.4 °C. According to Dhansay et al. (2017), the estimated geothermal gradient of each spring was based either on 'thermodynamics' (implying that the gradient was estimated from an inferred reservoir depth, based on existing geophysical data, surrounding heat flow and downhole temperature data, or on 'geothermometry' (i.e., using solute-based (silica or sodium-potassium) hydrochemical data.

Because the average temperature of the thermal springs in South Africa is $<$ 100 °C, namely 39.4 °C, which indicates likelihood of low-enthalpy geothermal resources (Dhansay et al., 2017), and because such resources are mostly associated with high-heat-producing radiogenic elements in granitoids (e.g., Siégel et al., 2014; Singh et al., 2020; Lacasse et al., 2022), the thermal springs' spatial relationship with high-heat-producing granitoids (denoted as HHPGs) (Fig. 2a) was investigated. This map of HHPGs was compiled/extracted from the 1:1,000,000 scale geological map of South Africa, which is freely available from the website of the Council for Geoscience of South Africa (https://www.geoscience.org.za). These HHPGs, according to Dhansay et al. (2017), are comprised mainly of the Cape granitoids (ca. 540 Ma (Browning and Macey, 2015), with highest relative heat production based on uranium concentration), Namaqualand granitoids (ca. 1100 Ma (cf. Clifford et al., 1975; Botha et al., 1979), with intermediate relative heat production based on uranium concentration), and Limpopo granitoids (ca. 2023–2595 Ma (McCourt & Armstrong, 1998), with lowest relative heat production based on uranium concentration).

In addition, because it is intuitive that thermal springs occurrence requires availability of groundwater, the thermal springs spatial relationship with groundwater yield was investigated. For this, a 1:1,000,000 scale map of classified groundwater yield over the whole of South Africa (Fig. 2b) was obtained from the South African Department of Water Affairs. Moreover, because it is intuitive that most (if not all) thermal springs are associated with faults/fractures that penetrate from

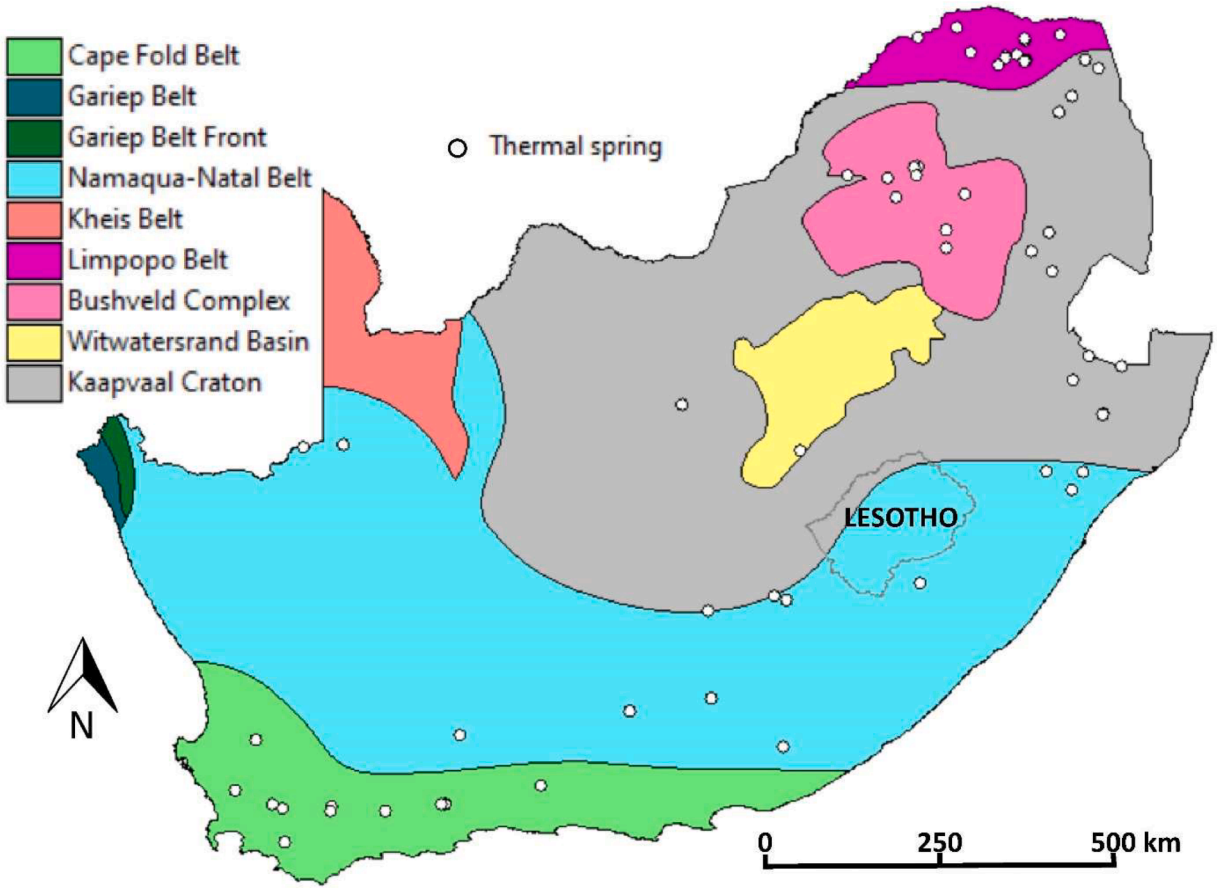

Fig. 1. Simplified regional geological map of South Africa showing the major litho-tectonic units and locations of thermal springs (adapted from Dhansay et al., 2017). (For interpretation of the references to colour in this figure legend, the reader is referred to the web version of this article).

certain depths in the subsurface to the ground surface, their spatial relationships with geological lineaments were investigated. For this, a 1:1,000,000 scale map of lineaments (Fig. 2c) was obtained from Jelsma et al. (2004); this map of lineaments was used instead of a 1:1,000,000 scale map of regional structures (shown as Fig. 2 in Dhansay et al., 2017) because the latter shows sparse regional structures of various types, which would undermine the accuracy of investigation of their spatial relationships with the thermal springs.

3.2. Investigation of spatial distribution

3.2.1. Point distribution analysis

Point spatial distributions can be categorized into three rudimentary kinds (Boots and Getis, 1988):

- Point distribution with complete spatial randomness (CSR): the points are unrelated to one another genetically or spatially. This kind of point distribution implies objects that arise from unrelated processes that happen fortuitously.
- Clustered point distribution: the points apparently develop sets in contrast to those in a distribution of points with CSR. This kind of point distribution implies objects that arise from an interaction of processes that lead to 'focusing' of sets of those objects into specific sites.
- Regular point distribution: the points are apparently farther apart from one another in contrast to those in a distribution of points with CSR. This kind of point distribution implies objects that arise from an interaction of processes that lead to 'spreading' of those objects into specific sites.

A point distribution that is being investigated is contrasted to one with CSR. The null hypothesis of such investigation is that the former point distribution possesses CSR, or that the objects proxied by the points are spatially unrelated to one another and every object is a product of a random process. The simplest alternate hypothesis is that the investigated point distribution does not possess CSR, or that the objects proxied by the points are related to one another, as they all arose from an interaction of particular processes. Therefore, if existing thermal springs depicted as points on a map are distributed non-randomly, that is because they are due an interaction of certain geological processes, then they may exhibit either a clustered or a regular distribution. The null and/or alternate hypotheses can be investigated through various techniques, which can be classified largely into two kinds of analyses (Boots and Getis, 1988): (a) dispersion analysis; and (b) arrangement analysis.

In a dispersion analysis, observed distances between point pairs are contrasted with expected distances between point pairs in a distribution with CSR (Boots and Getis, 1988). In a point distribution being investigated, the number of points is denoted as p, and observed distances between point pairs are denoted as first-, second-, third- or $(p-1)$ th-order distances; the first-order distance is the closest distance. A point distribution with CSR is simulated with equal area and equal number of points as the point distribution being investigated. If the average of observed pth-order distances is lesser compared to the average of expected pth-order distances in CSR, the point distribution under investigation is clustered. If the average of observed pth-order distances is greater compared to the average of expected pth-order distances in CSR, the point distribution being investigated is regular. Whether the average of observed and average of expected nth-order distances are significantly different or not may be verified statistically under the assumption

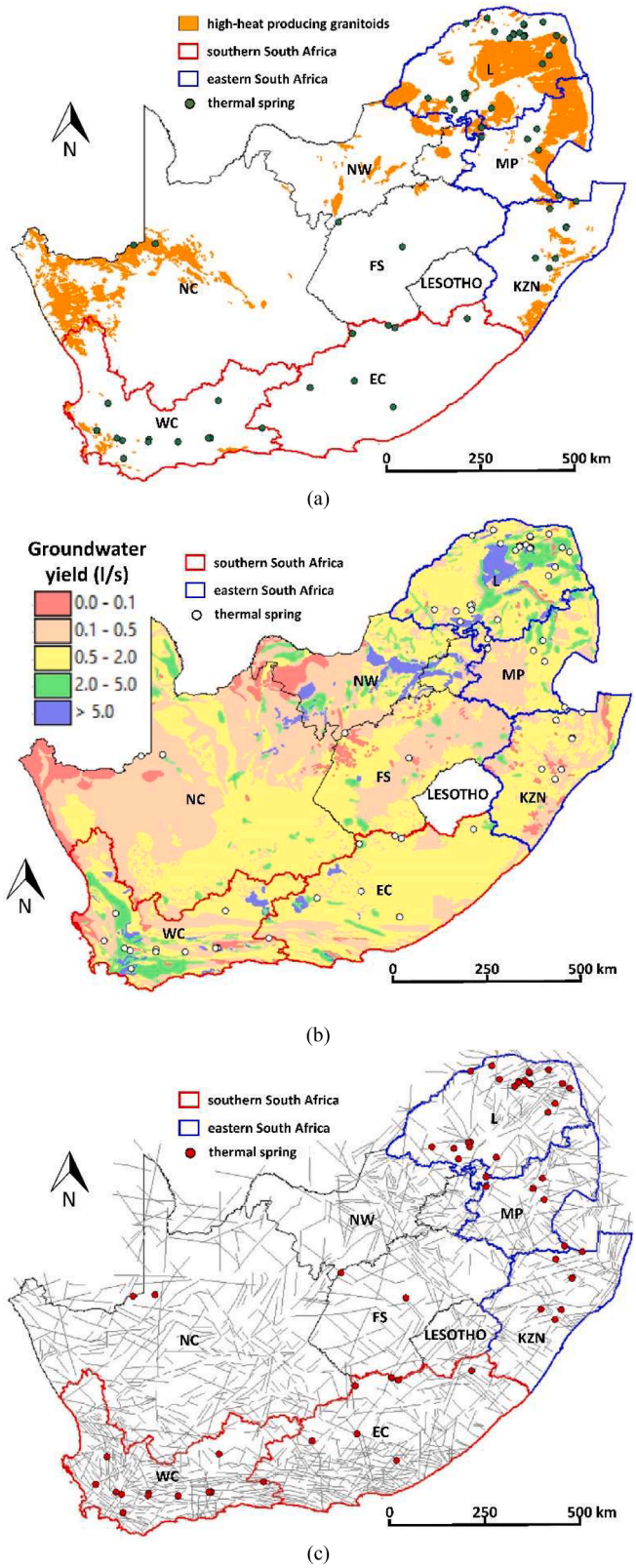

Fig. 2. Geological features considered for analyses of spatial relationships with thermal springs in South Africa: (a) high-heat-producing granitoids (adapted from Council for Geoscience), (b) groundwater yield (adapted from South African Department of Water Affairs), and (c) lineaments (grey lines) interpreted from digital elevation images (adopted from Fig. 3b of Jelsma et al., 2004). (For interpretation of the references to colour in this figure legend, the reader is referred to the web version of this article).

of normal distribution. Details of dispersion analysis can be found in Boots and Getis (1988).

In arrangement analysis, the number of observed reciprocal closest neighbor points (RCNPs) in a point distribution being investigated is contrasted with the number of expected RCNPs in a point distribution with CSR (Boots and Getis, 1988). A point distribution with CSR is simulated with equal area and equal number of points as the point distribution being investigated. Pairs of points in a point distribution are regarded as first-order RCNPs as long as they are the closest neighbor of each other in a locality of points, as second-order RCNPs as long as they are second-closest neighbors of each other in a locality of points, and so on. RCNPs are point pairs all the time; thus, the number of observed RCNPs is an even number all the time. The number of expected *n*th-order RCNPs is approximated based on the likelihood that a point in a point distribution with CSR is the *n*th-closest neighbor of its own *n*th-closest neighbor (Cox, 1981). If the number of observed *n*th-order RCNPs is larger compared to the number of expected *n*th-order RCNPs in a point distribution with CSR, the point distribution under investigation is clustered. If the number of observed *n*th-order RCNPs is smaller compared to the number of expected *n*th-order RCNPs in a point distribution with CSR, the point distribution being investigated is regular. However, Boots and Getis (1988) pointed out that no statistical tests exist to determine whether the difference between the numbers of observed and expected *n*th-order RCNPs is significant or not.

Point distribution analysis has been used by several researchers to deduce geological controls on mineralization (e.g., Carranza, 2009; Zheng et al., 2020; Sadigh et al., 2022). Here, we used the GIS and remote sensing software ILWIS 3.3 Academic for point distribution analysis of thermal springs in South Africa in order to aid deducing the geological controls on their occurrence.

3.2.2. Fractal analysis

The term fractal was introduced by Mandelbrot (1982) to describe a geometric figure that consists of parts that possess geometries (e.g., form, shape), aside from scale or size, which are alike to the whole figure. A geometric figure is regarded as a fractal if its dimension (denoted as FD) exceeds its Euclidean dimension (denoted as ED). Thus, a fractal point has a FD within the range from 0 (ED of a point) to 1 (ED of a line). Likewise, a fractal line does not have ED = 1 but has a FD within the range from 1 to 2 (ED of an area), a fractal area has a FD within the range from 2 to 3 (ED of a volume), a fractal volume has a FD larger than 3, and so on.

The FD of a point distribution is quantifiable by the box-counting technique, whereby a regular grid of square cells with size d (= side of a cell) is placed on a point distribution map. The number of cells, $n(d)$, with at least one point is counted. This process is iterated for different cell sizes d and the findings are plotted on a log–log graph, with d on the x-axis and $n(d)$ on the y-axis. According to Mandelbrot (1985), a point distribution is a fractal if the log–log plots of $n(d)$ vs. d can be fitted with a power–law function, thus (cf. Carlson, 1991):

$$n(d) = cd^{-FD_b} \quad (1)$$

where FD_b is the slope of a line fitted by least squares method to the log–log plots of $n(d)$ vs. d, and c is a constant denoting a measure of proportionality between $n(d)$ and d. The FD_b is a proxy measure of the FD of a point distribution. For a random point distribution, the slope of the line fitted log–log plots of $n(d)$ vs. d is -2; for a fractal point distribution, the slope varies in the range from 0 to -2. The box-count FD is the absolute value of FD_b. The $n(d)$ vs. d relationship in Eq. (1) has been applied by various researchers to investigate the spatial distribution of diverse types of mineral deposits to deduce geological controls on their occurrence (e.g., Carlson, 1991; Cheng et al., 1996; Weiberg et al., 2004; Ford and Blenkinsop, 2008). Here, we used the GIS and remote sensing software ILWIS 3.3 Academic for fractal analysis based on Eq. (1) to aid deducing the geological controls on thermal springs occurrence in South

Africa. In a raster-based GIS like ILWIS, the box-counting technique entails (a) rasterizing the point locations of thermal springs with different pixel (or cell) sizes (d) to determine the count of pixels (or cells) where thermal springs exist [$n(d)$]. Then, we used Excel to plot $n(d)$ vs. d and determine FD_b.

3.2.3. Fry analysis

Fry analysis (Fry, 1979) plots translations of a set of points by treating every single point as a center (or origin) for translation. This can be done manually by having a transparent sheet with the positions of all the original points, a denoted center for translation and a reference line. A second transparent sheet is prepared with all the points, a denoted center for translation and a reference line like in the first sheet. The center for translation on the second transparent sheet is then overlaid on one point of the first sheet, then the positions of all the points in the first sheet are denoted on the second sheet. The center for translation on the second transparent sheet is overlaid again on a different point in the first sheet, then the positions of all the points in the first sheet are denoted on the second sheet. By doing this until all the points are used as centers for translation, an original distribution with p number of points yields is enhanced into a Fry plot with p^2–p number of points, which can be used for further trend analysis (Fry, 1979).

Complementary rose diagrams can be created for the Fry analysis results in order to visualize the orientations of every pair of Fry points. Rose diagrams can be generated for analysis of orientation data for (a) all Fry point pairs and (b) Fry point pairs at specific distances from one another. Orientations in analysis (a) can be attributed to regional-scale geological factors, while orientations in analysis (b) can be ascribed to district-scale geological factors. For orientation analysis (a), the minimum distance between Fry point pairs where there is the highest probability of finding at least one point next to another is specified. This minimum distance is obtained from point distribution analysis where the probability that at least one point exists next to another point is calculated as a function of distance (Boots and Getis, 1988).

As mentioned in the Introduction, Fry analysis has been applied by several researchers (e.g., Carranza et al., 2008; Moghaddam et al., 2013, 2014; Sang et al., 2017) to describe the regional-scale spatial distributions of thermal springs elsewhere. Here, we used the free DotProc software for Fry analysis to aid deducing the geological controls on thermal springs' occurrence in South Africa. The point coordinates of the thermal springs stored in ILWIS 3.3 Academic were exported to DotProc. The coordinates of Fry points generated by DotProc were then exported into ILWIS 3.3 Academic for visualizing and investigating together the spatial distributions of the Fry plots and the thermal springs. The output file of trends of every pair of Fry points generated by DotProc was also exported into the free GeoRose software to create rose diagrams.

3.3. Investigation of spatial relationship

As discussed in the Introduction section, distance distribution analysis was used in this study to investigate the regional-scale spatial relationships of thermal springs with specific relevant geological features. The distance distribution analysis used here to investigate the spatial relationship of a distribution of points with a set of other geometric features is adapted from Berman (1977, 1986). The distance distribution analysis has been employed by Ghosh and Carranza (2010) and Gorum and Carranza (2015) to investigate the spatial relationships of landslide occurrences with various geological features. The description of the distance distribution analysis given below is modified from Carranza (2009).

The distance distribution analysis entails a comparison of an accumulative relative frequency of distances from a set of geometric figures to individual points in the point distribution being investigated (denoted as $D(I)$) and an accumulative relative frequency of distances from the same set of geometric figures to all locations in the same area covered by the point distribution (denoted as $D(R)$). The $D(I)$ is assumed to be a non-random distribution of points of interest based on the geometric figures and the $D(R)$ portrays a random distribution of all locations based on the same geometric figures. The null hypothesis of this analysis, which can be tested by comparing the plots $D(I)$ and $D(R)$, is that the point distribution being investigated lacks spatial relationship with the set of geometric figures.

If the $D(I)$ plot follows the $D(R)$ plot closely, the points of interest are distributed randomly with respect to the geometric figures. If the $D(I)$ plot lies above the $D(I)$ plot (i.e., a positive $D(I)$–$D(R)$ difference), the point distribution being investigated possess positive spatial relationship with the geometric figures; if not, they possess negative spatial relationship. A positive $D(I)$–$D(R)$ difference (denoted as D) depicts a chance of occurrence of the points of interest that is higher than a random chance as a function of distance from the geometric figures. The magnitude of D reflects the strength or weakness of the positive spatial relationship of the points of interest with the geometric figures being investigated. Geometric figures with which a point distribution has strong positive spatial relationship represent a spatial control on the occurrence of the points of interest. The highest peak in a plot of D corresponds to a distance from the geometric figures within which the positive spatial relationship of the points of interest with the geometric figures is optimum. The magnitude of the ratio of $D(I)$ to $D(R)$ at the distance of optimum positive spatial relationship of the points of interest with the geometric figures is a measure of the relative strength of the spatial relationship; this ratio allows comparing the relative strengths of the spatial relationships of the points of interest with different sets of geometric features.

For the investigations of the thermal springs' spatial relationships with geological lineaments, the latter were grouped according to six general orientations (i.e., ENE (i.e., 60°–90°), NE (i.e., 30°–60°), NNE (i.e., 0°–30°), NNW (i.e., 330°–360°), NW (i.e., 300°–330°), WNW (i.e., 270°–300°)) because it can be expected that not all sets of geological lineaments based on orientation are associated with thermal springs, as indicated by the Fry analyses above. For example, several thermal springs in the Cape Fold Belt in southern South Africa are linked to ENE-trending faults (Diamond and Harris, 2000; Madi et al., 2016). Similarly, certain thermal springs in KwaZulu-Natal in eastern South Africa are associated with ENE-trending faults (Gravelet-Blondin, 2013). In addition, it can be expected that not all sets of geological lineaments based on orientation are associated with the heat and/or water sources of the thermal springs. For example, Du Plessis and Walraven (1990) concluded that the ENE-trending Thabazimbi–Murchison lineament controlled the emplacement of the Bushveld Complex, which comprise some of the HHPGs in eastern South Africa (Figs. 1, 7a). Also, Abiye et al. (2020) found that ENE-trending tectonic lineaments and dolerite dikes dictate the groundwater flow pattern in the Hout River Catchment, Limpopo province, in eastern South Africa.

4. Results

The investigations of the thermal springs' spatial distribution and their spatial relationships with geological features were carried out over the whole of South Africa. However, as noted in Section 2 above, there is an apparent geographic and geologic control on the thermal springs' spatial distribution. As can be seen in Fig. 1, many thermal springs are distributed in southern part of the country where they exist on the Namaqua-Natal and Cape Fold Belts, and many thermal springs are distributed in the eastern part of the country where they exist on the Kaapvaal Craton, Limpopo Belt and Bushveld Complex. Therefore, it is instructive to investigate the thermal springs' spatial distribution and their spatial relationships with geological features separately in the southern and eastern parts of the country. Because there is no obvious geological basis for drawing the boundary of the southern and eastern parts with rest of the country, we used the administrative boundaries of South Africa's provinces to delineate the southern and eastern parts of the country for the purpose of the investigations (Fig. 3). However, a

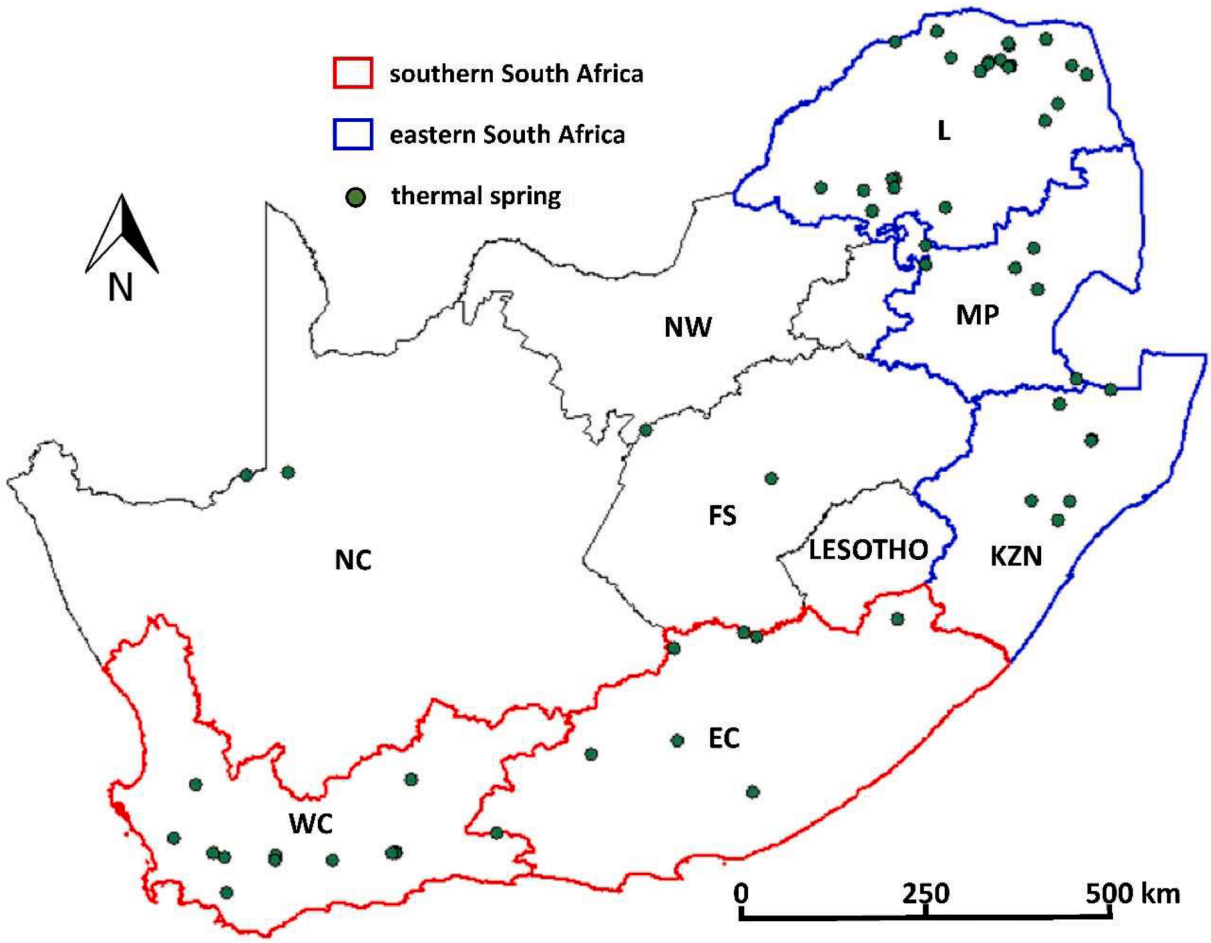

Fig. 3. Division of South Africa into a southern part and an eastern part based on boundaries of administrative provinces to supplement the investigation of the thermal springs' spatial distribution and their spatial relationships with geological features over the whole of the country. WC = Western Cape. EC = Eastern Cape. KZN = KwaZulu-Natal. MP = Mpumalanga. L = Limpopo. NW = North West. FS = Free State. NC = Northern Cape. (For interpretation of the references to colour in this figure legend, the reader is referred to the web version of this article).

long section of the Vaal River forms the boundary of the Free State province with the provinces of Northwest, Gauteng and Mpumalanga whereas a short section of the Orange River forms the boundary of the Free State province with the provinces of Northern Cape and Eastern Cape. The rough correlations of the administrative boundaries of South Africa's provinces with topographical or geomorphological features, like major rivers, somehow justify using them to delineate the southern and eastern parts of the country for the purpose of the investigations. Thus, southern South Africa pertains to the provinces of Western Cape and Eastern Cape, where 20 thermal springs exist on the Namaqua-Natal and Cape Fold Belts, and eastern South Africa pertains to the provinces of KwaZulu-Natal, Mpumalanga and Limpopo, where 33 thermal springs exist on the Kaapvaal Craton, Limpopo Belt and Bushveld Complex (Figs. 1 and 2). Performing the investigation per litho-tectonic unit (Fig. 1) was not considered because structures that may have controlled the thermal springs' occurrence in the country likely cut through different litho-tectonic units.

4.1. Investigation of spatial distribution of thermal springs

4.1.1. Point distribution analysis

Based on the dispersion analysis, the distribution of thermal springs in the whole of South Africa is clustered because the averages of observed first- to sixth-order neighbor distances in their distribution are smaller than the corresponding averages of expected first- to sixth-order neighbor distances in a point distribution with CSR (Table 1). However, based on the arrangement analysis, only the observed number of first-order RCNPs of the thermal springs exceeded the expected number of first-order RCNPs of a point distribution with CSR, indicating a clustered distribution; the observed and expected numbers of lower-order RCNPs indicate a regular distribution (Table 2). Thus, based on both the dispersion and arrangement analyses, the spatial distribution of thermal springs in the whole of South Africa is largely clustered and partly regular.

Table 1
Results of dispersion analysis of the thermal springs' spatial distribution in the whole of South Africa.

Order	Averages of neighbor distances (km)	
	Observed	Expected in CSR
1	45.6	85.6
2	83.4	127.8
3	108.9	160.0
4	125.6	186.7
5	142.3	210.1
6	167.8	231.2

Based on the dispersion analysis, the thermal springs' distribution in southern South Africa is clustered because the averages of observed first- to sixth-order neighbor distances in their distribution are smaller than the corresponding averages of expected first- to sixth-order neighbor distances in a point distribution with CSR (Table 3). However, based on

Table 2
Results of arrangement analysis of the thermal springs' spatial distribution in the whole South Africa.

Order	Number of RCNPs	
	Observed	Expected in CSR
1	42	39.8
2	18	21.1
3	12	15.6
4	8	12.9
5	8	11.3
6	6	10.1

Table 3
Results of dispersion analysis of the thermal springs' spatial distribution in southern South Africa.

Order	Averages of neighbor distances (km)	
	Observed	Expected in CSR
1	70.0	75.6
2	103.4	113.4
3	136.7	142.3
4	158.9	165.6
5	178.9	186.7
6	232.3	205.6

the arrangement analysis, the thermal springs' distribution in southern Africa is mostly regular because only the observed number of sixth-order RCNPs of the thermal springs exceeded the corresponding expected number of sixth-order RCNPs of a point distribution with CSR, which indicate a clustered distribution (Table 4). Thus, based on both the dispersion and arrangement analyses, the thermal springs' distribution in the whole of South Africa is largely clustered and partly regular.

Based on the dispersion analysis, the distribution of thermal springs in eastern South Africa is clustered because the averages of observed first- to sixth-order neighbor distances in their distribution are smaller than the corresponding averages of expected first- to sixth-order neighbor distances in a point distribution with CSR (Table 5). However, based on the arrangement analysis, only the observed numbers of first- to second-order RCNPs of the thermal springs exceeded the corresponding expected numbers of first- to second-order RCNPs of a point distribution with CSR, indicating a clustered distribution; the observed and expected numbers of lower-order RCNPs indicate a regular distribution (Table 6). Thus, based on both the dispersion and arrangement analyses, the spatial distribution of thermal springs in eastern of South Africa is largely clustered and partly regular.

4.1.2. Fractal analysis

The spatial distribution of the existing thermal springs in the whole of South Africa has two box-counting FDs, as two straight lines, separated at $d = 100$ km, fit the log–log plots of $n(d)$ vs. d almost perfectly (Fig. 4a). The slope of the straight line fitted through plots for $d \leq 100$ km is -0.066 (i.e., $FD_b = 0.066$), whereas that for the one fitted through plots for $d \geq 100$ km is -1.192 (i.e., $FD_b = 1.091$). Likewise, the spatial distribution of the existing thermal springs in southern South Africa has

Table 4
Results of arrangement analysis of the thermal springs' spatial distribution in southern South Africa.

Order	Number of RCNPs	
	Observed	Expected in CSR
1	10	12.43
2	4	6.58
3	4	4.86
4	2	4.03
5	2	3.52
6	4	3.16

Table 5
Results of dispersion analysis of the thermal springs' spatial distribution in eastern South Africa.

Order	Averages of neighbor distances (km)	
	Observed	Expected in CSR
1	30.0	47.8
2	48.9	71.1
3	72.2	90.0
4	81.1	104.5
5	98.9	117.8
6	114.5	128.9

Table 6
Results of arrangement analysis of the thermal springs' spatial distribution in eastern South Africa.

Order	Number of RCNPs	
	Observed	Expected in CSR
1	26	22.37
2	12	11.85
3	8	8.75
4	4	7.25
5	2	6.34
6	4	5.70

two box-counting FDs, as two straight lines, separated at $d = 100$ km, fit the log–log plots of $n(d)$ vs. d almost perfectly (Fig. 4b). The slope of the straight line fitted through plots for $d \leq 100$ km is -0.077 (i.e., $FD_b = 0.077$), whereas that for the one fitted through plots for $d \geq 100$ km is -0.833 (i.e., $FD_b = 0.833$). Similarly, the spatial distribution of the existing thermal springs in eastern South Africa has two box-counting FDs, as two straight lines, separated at $d = 50$ km, fit the log–log plots of $n(d)$ vs. d almost perfectly (Fig. 4c). The slope of the straight line fitted through plots for $d \leq 50$ km is -0.071 (i.e., $FD_b = 0.071$), whereas that for the one fitted through plots for $d \geq 50$ km is -0.857 (i.e., $FD_b = 0.857$).

Because none of the slopes of the fitted lines was equal to -2, which is the slope of a line fitted through log–log plots of $n(d)$ vs. d for a random point distribution, the results indicate that the spatial distributions of thermal springs in the whole, southern and eastern South Africa are non-random. Whether the spatial distribution of the thermal springs under investigation is clustered or not can be deduced from the values of FD_b. Note that a point and a line have Euclidean dimensions of 0 and 1, respectively. Now, the values of FD_b at shorter distances or smaller spatial scales (i.e., $d \leq 100$ km for the whole and southern South Africa, and $d \leq 50$ km for eastern South Africa) are remarkably close to 0. This implies that, at spatial scales of $d \leq 100$ km, the thermal springs behave like points, meaning that they are focused (or clustered) at certain locations but not spread out to certain locations. In contrast, the values of FD_b at longer distances or larger spatial scales (i.e., $d \geq 100$ km for the whole and southern South Africa, and $d \geq 50$ km for eastern South Africa) are quite close to 1. This implies that, at spatial scales of $d \geq 50$ km, the thermal springs behave less like points but more like lines, meaning that they are oriented (or are spread) along certain linear trends. The overall interpretation of the two box-counting FDs at two spatial scales is that the thermal springs form clusters at spatial scales of $d \leq 100$ km and that these clusters of thermal springs follow certain linear trends at spatial scales of $d \geq 50$.

In southern South Africa, the clustering of the thermal springs is within a spatial scale of 100 whereas in eastern South Africa the clustering of the thermal springs is within a spatial of 50 km.

4.1.3. Fry analysis

Table 7 summarizes the trends depicted by Fry plots of thermal springs in South Africa, whereas Figs. 5 to 7 illustrates these trends.

Fig. 5a shows the Fry plot of the 64 thermal springs in the whole South Africa. The major trend of all pairs of Fry points of thermal springs

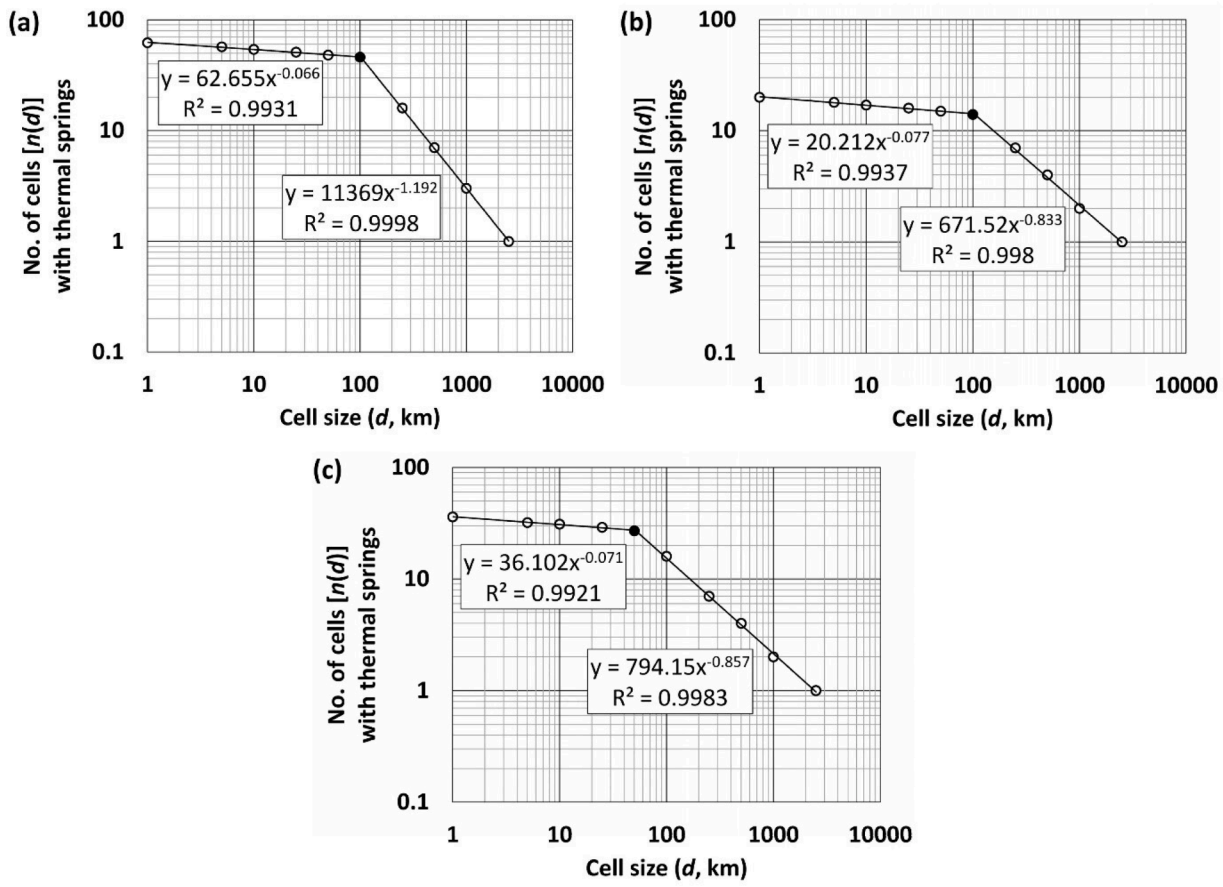

Fig. 4. Log–log plots (white and black dots) defining the following relation of $n(d)$ vs. d for the thermal springs' spatial distribution in (a) the whole of South Africa, (b) southern South Africa, and (c) eastern South Africa. See Fig. 3 for the locations of thermal springs in these areas.

Table 7
Summary of trends depicted by Fry plots of thermal springs in South Africa. Trends in bold are common at regional- and district-scales in the whole of South Africa or at district- and local-scales in southern or eastern South Africa.

Region/District	Regional-scale trend(s)		District-scale trend(s)		Local-scale trend(s)	
	Major	Minor	Major	Minor	Major	Minor
Whole of South Africa	**NE–SW**	NNW–SSE, **ENE–WSW**	WNW–ESE	NW–SE, **ENE–WSW**, **NE–SW**		
Southern South Africa			**ENE–WSW**		**ENE–WSW**	
Eastern South Africa			**NNW–SSE**	**NE–SW**	**NE–SW**	WNW–ESE, ENE–WSW, **NNW–SSE**

in the whole country is NE–SW (i.e., 30°–60° or 210°–240°) (Fig. 5b, Table 7). This regional-scale trend in the thermal springs' spatial distribution in the whole of South Africa may somehow be influenced by the NE–SW trend of the country's long axis (Fig. 5a), or it may be related to regional-scale NE–SW-trending linear geological structures. There are also minor regional-scale NNW–SSE (i.e., 330°–360° or 150°–180°) and ENE–WSW (i.e., 60°–90° or 240°–270°) trends among all pairs of Fry points of thermal springs in the whole country (Fig. 5a, Table 7). In contrast, for Fry point pairs within 220 km of each other (i.e., the minimum distance from any thermal spring within which there is maximum probability that at least one thermal spring exists next to it), the major district-scale trend is WNW–ESE (i.e., 270°–300° or 90°–120°) (Fig. 5c, Table 7), which may be related district-scale WNW–ESE-trending linear geological structures. However, there is a minor district-scale NE–SW trend among the Fry point pairs within 220 km of each other (Fig. 5c), suggesting that some of the thermal springs in the whole of South Africa may be related to regional-scale NE–SW-trending linear geological structures. There is also a minor NW–SE (i.e., 300°–330° or 120°–150°) district-scale trend among the Fry point pairs within 220 km of each other (Fig. 5c), suggesting that some thermal springs in the whole of South Africa may be related to district-scale NW–SE-trending linear geological structures.

Fig. 6a shows the Fry plot of the 36 thermal springs in southern South Africa. The major trend of all pairs of Fry points of thermal springs in this district is ENE–WSW (Fig. 6b). This district-scale trend in the thermal springs' spatial distribution in southern South Africa may be influenced by the ENE–WSW trend of this region's long axis (Fig. 6a), or it may be related to district-scale ENE–WSW-trending linear structures in this district. However, a major local-scale ENE–WSW trend is exhibited by Fry point pairs within 220 km of each other (i.e., the minimum distance from any thermal spring within which there is maximum probability that at least one thermal spring exists next to it) (Fig. 6c). Therefore, the major district- and local-scale ENE–WSW trends in the Fry plot of the thermal springs in southern South Africa is likely due to geological controls rather than to the shape of this district.

Fig. 7a shows the Fry plot of the 36 thermal springs in eastern South Africa. The major trend of all pairs of Fry plots for thermal springs in this district is NNW–SSE (Fig. 7b, Table 7). This district-scale trend in the

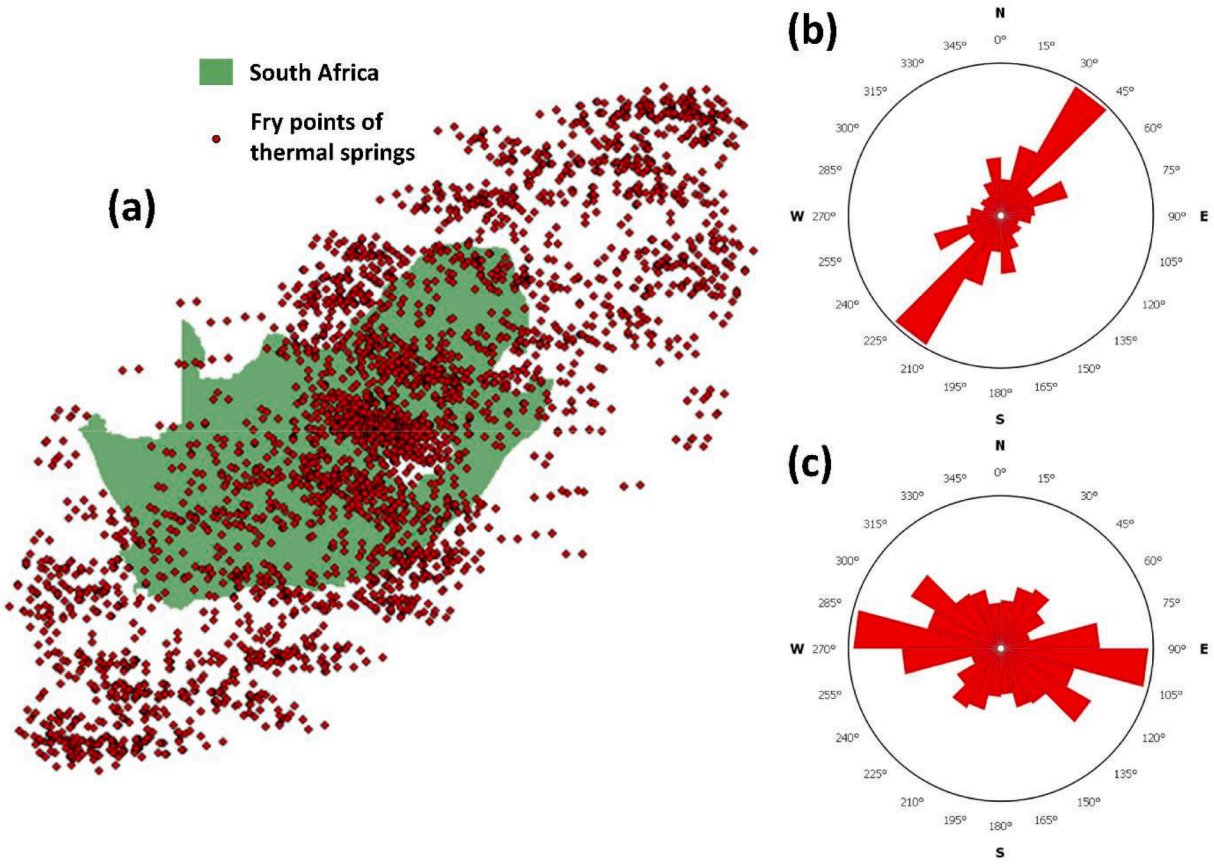

Fig. 5. Spatial distribution of 64 thermal springs in the whole of South Africa: (a) Fry plot; (b) rose diagrams of trends among all Fry point pairs in (a); (c) rose diagrams of trends among Fry point pairs within 220 km of each other (i.e., the minimum distance from any thermal spring within which there is maximum probability that at least one thermal spring exists next to it). (For interpretation of the references to colour in this figure legend, the reader is referred to the web version of this article).

thermal springs' spatial distribution in eastern South Africa may be influenced by the NNW–SSE trend of this region's long axis (Fig. 7a), or it may be related to district-scale NNW–SSE-trending linear geological structures in this district. There is also a minor district-scale NE–SW trend among all pairs of Fry plots for thermal springs in this district (Fig. 7b, Table 7). In contrast, for Fry point pairs within 67 km of each other (i.e., the minimum distance from any thermal spring in this district within which there is maximum probability that at least one thermal spring exists next to it), the major trend is NE–SW (Fig. 5c, Table 7). This major local-scale NE–SW trend in the thermal springs' spatial distribution in eastern South Africa, which is also a minor district-scale trend (Fig. 7b, Table 7), may be related mostly to local-scale and partly to district-scale NE–SW-trending linear geological structures in this district. However, there is a minor local-scale NNW–SSE trend among the Fry point pairs within 67 km of each other (Fig. 7c). This minor local-scale NNW–SSE trend, which is also the major district-scale trend (Fig. 7b, Table 7), suggests that some of the thermal springs in eastern South Africa may be related mostly to local-scale and partly to district-scale NNW–SSE-trending linear geological structures in this district. There is also a minor WNW–SSE to ENE–WSW local-scale trend among the Fry point pairs within 67 km of each other (Fig. 7c), suggesting that some thermal springs in eastern South Africa may be related to local-scale WNW–SSE-trending linear geological structures in this district.

4.2. Investigation of spatial relationships of thermal springs with geological features

4.2.1. Thermal springs vs. high-heat-producing granitoids

The thermal springs in South Africa have positive spatial relationships with HHPGs (Figs. 8a, 9a, 10a). According to Table 8, at regional- to district-scales, about 53 % to 100 % of the known thermal springs in South Africa exists within 39–46 km of an HHPG. The thermal springs' positive spatial relationships with HHPGs in southern and the whole South Africa are stronger than in eastern South Africa (Table 8).

4.2.2. Thermal springs vs. groundwater yield

The thermal springs in South Africa have positive spatial relationships with groundwater yield (Figs. 8b, 9b, 10b). According to Table 9, at regional- to district-scales, about 90 % to 94 % of the known thermal springs in South Africa exists where there is at least 2 L/s of groundwater yield. This finding supports the findings of the point distribution analysis and fractal analysis that the thermal springs' spatial distribution in South Africa is not random. The thermal springs' positive spatial relationships with groundwater yield in eastern and southern South Africa are weaker than in the whole of South Africa (Table 9), and the thermal springs' positive spatial relationship with HHPGs in southern South Africa is weaker than in eastern South Africa.

4.2.3. Thermal springs vs. ENE-trending geological lineaments

Among all the thermal springs in South Africa, only ENE-trending lineaments have positive spatial relationships with thermal springs in the whole of South Africa (Figs. 8–10). According to Table 10, at regional- to district-scales, about 74 % to 81 % of the known thermal springs in South Africa exists within 19 km of an ENE-trending lineament. The thermal springs' positive spatial relationships with ENE-trending lineaments is strongest in the whole of South Africa, intermediate in southern South Africa, and weakest in eastern South Africa (Table 10).

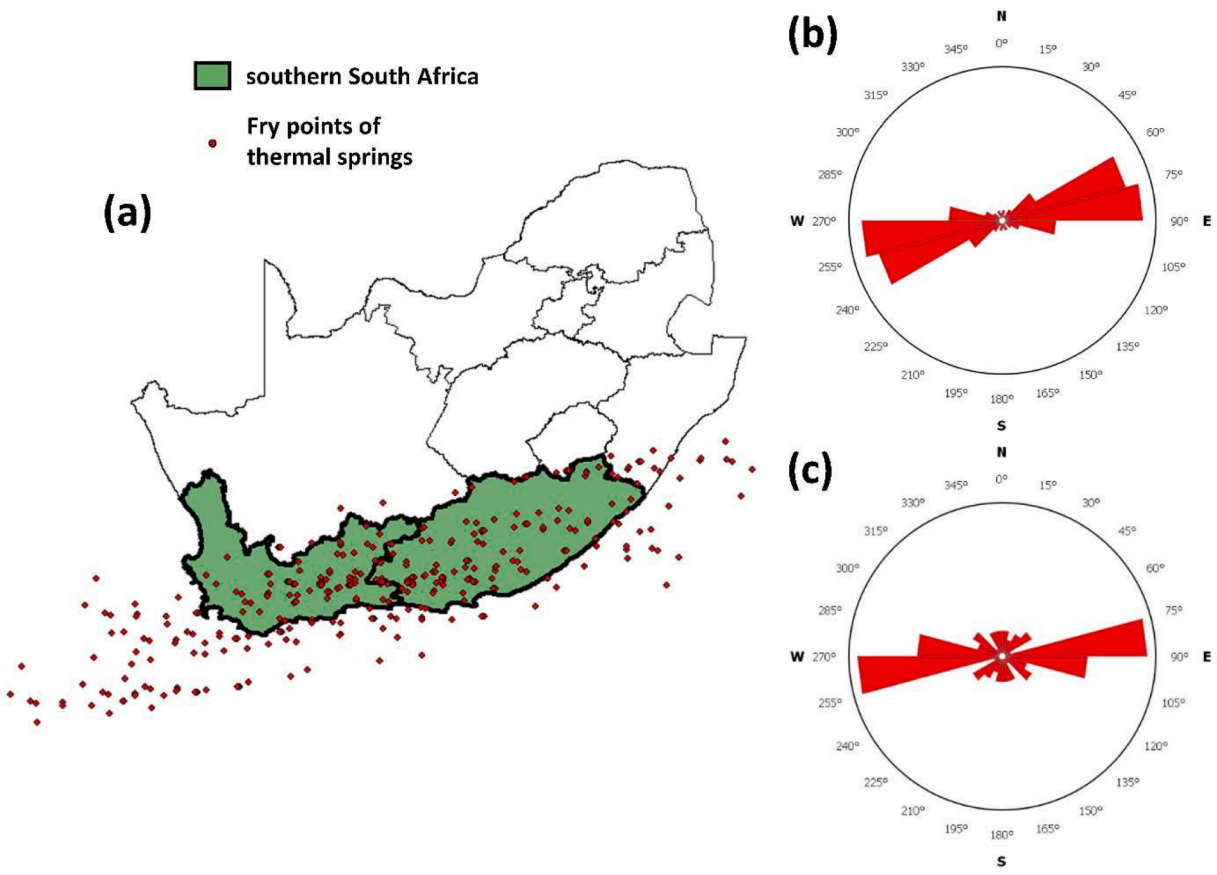

Fig. 6. Spatial distribution of 20 thermal springs in southern South Africa: (a) Fry plot; (b) rose diagram of trends among all Fry point pairs in (a); (c) rose diagram of trends among Fry point pairs within 220 km of each other (i.e., the minimum distance from any thermal spring within which there is maximum probability that at least one thermal spring exists next to it). (For interpretation of the references to colour in this figure legend, the reader is referred to the web version of this article).

4.2.3. Thermal springs vs. other sets of geological lineaments

Among the remaining sets of geological lineaments based on orientation, WNW-trending lineaments have positive spatial relationships with thermal springs in the whole of South Africa and in eastern South Africa (Figs. 8h, 10h) but they have mostly independent spatial relationship with thermal springs in southern South Africa (Fig. 9h). According to Table 11, at regional- to district-scales, about 82 %t to 89 % of the known thermal springs in South Africa, especially in eastern South Africa, exists within 39 km of a WNW-trending lineament. The thermal springs' positive spatial relationships with WNW-trending lineaments is stronger in eastern South Africa than in the whole South Africa (Table 11). That is, in conjunction with the results of Fry analyses, WNW-trending lineaments impose a minor district- and local-scale WNW–ESE trend in the thermal springs' spatial distribution in eastern South Africa, but they do not impose a regional-scale WNW–ESE trend in the thermal springs' spatial distribution in the whole of South Africa (cf. Table 7).

NNW- and NW-trending lineaments have positive spatial relationships with thermal springs in southern South Africa (Fig. 9f, g) but not in the whole of South Africa and in eastern South Africa. This means that NNW- and NW-trending lineaments have controls on thermal spring occurrence in southern South Africa but not in other parts of South Africa. This further means that the major NNW–SSE trend in the Fry plot of thermal springs in eastern South Africa is not due to controls by NNW-trending lineaments but to the influence of the long axis of eastern South Africa. In southern South Africa, the optimum distance of positive spatial relationship between the thermal springs and NNW-trending lineaments is 29 km (Fig. 9f), whereas that between the thermal springs and NW-trending lineaments is 9 km (Fig. 9g); thus, the thermal springs have stronger positive spatial relationship with the latter set of lineaments compered to the former. However, these trends are not depicted by the Fry analyses in southern South Africa (Fig. 6), which reveal regional- and district-scale trends, and so NNW- and NW-trending lineaments only have local-scale controls on thermal spring occurrence in southern South Africa.

NNE- and NE-trending lineaments have either negative or independent spatial relationships with thermal springs in the whole of South Africa including its southern and eastern parts (Figs. 8d, 8e, 9d, 9e, 10d, 10e). There is no distinct NNE–SSW trend in the Fry plot of the thermal springs in the whole of South Africa (Fig. 5); therefore, the negative or independent spatial relationships of the thermal springs thermal springs with NNE-trending lineaments in the country is real. However, the presence of distinct NE–SW trends in the Fry plot of the thermal springs in the whole of South Africa (Fig. 5) and the negative or independent spatial relationships of the thermal springs thermal springs with NE-trending lineaments in the country indicate that the distinct NE–SW trends in the Fry plot of thermal springs in South Africa (Fig. 5) are not due to lineaments controls but to the general NE–SW long axis of the shape of the country. In contrast, the presence of major local-scale NE–SW trend in the Fry plot of the thermal springs in eastern South Africa (Fig. 7, Table 7) and the negative or independent spatial relationships of the thermal springs thermal springs with NE-trending lineaments in eastern South Africa suggest that that distinct NE–SW trend in the Fry plot of thermal springs is likely due to controls by local-scale linear structures, but the spatial relationship analysis made use of regional- to district-scale lineaments (Fig. 2c).

4.2.4. Thermal springs vs. intersections of geological lineaments

In southern South Africa, thermal springs have (a) strong positive spatial relationships with ENE-trending lineaments (Fig. 9c) weak

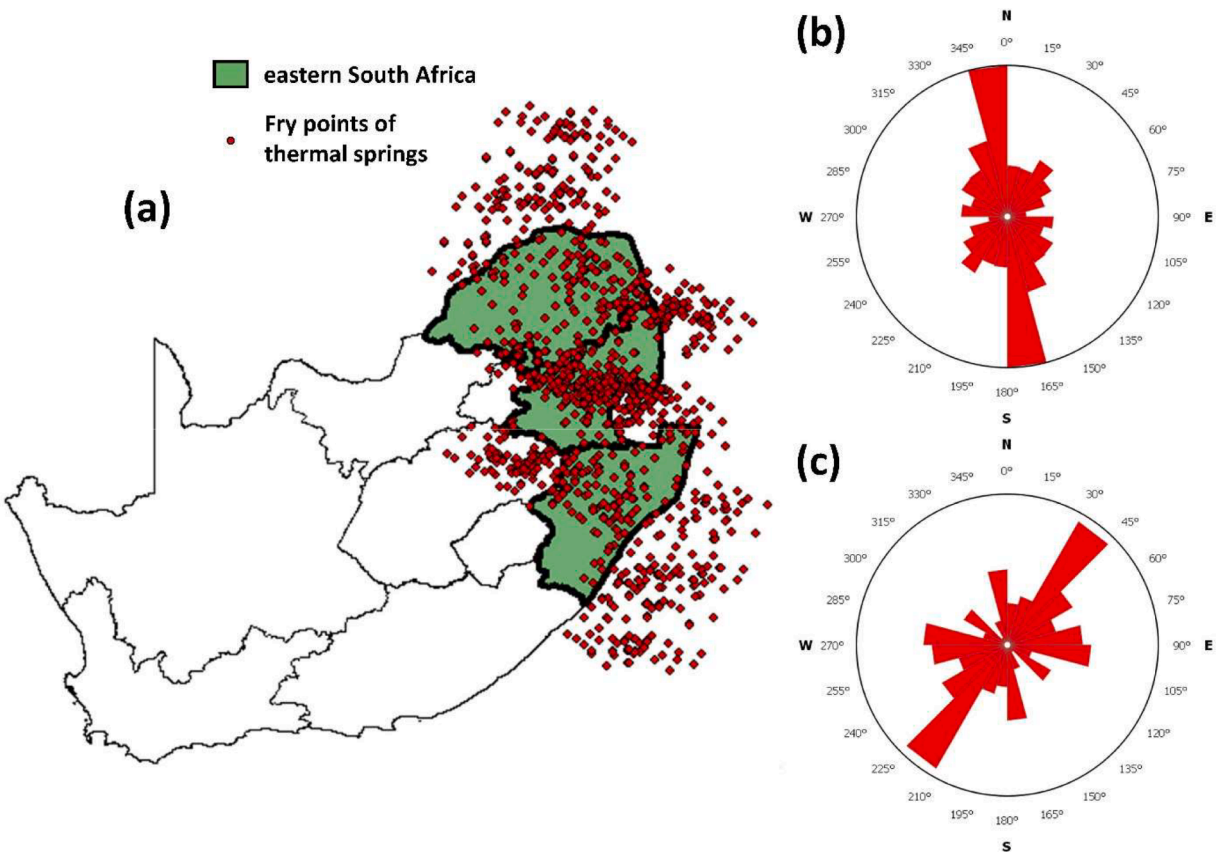

Fig. 7. Spatial distribution of 36 thermal springs in eastern South Africa: (a) Fry plot; (b) rose diagram of trends among all Fry point pairs in (a); (c) rose diagram of trends among Fry point pairs within 67 km of each other (i.e., the minimum distance from any thermal spring within which there is maximum probability that at least one thermal spring exists next to it). (For interpretation of the references to colour in this figure legend, the reader is referred to the web version of this article).

positive spatial relationships with NNW- and NW-trending lineaments (Fig. 9f, g), exhibit major ENE–WSW trend but even minor NNW–SSE and NW–SE trends in their Fry plot (Fig. 7, Table 7). These suggest that (a) thermal springs in southern South Africa have positive spatial relationship with intersections of NNW- and NW-trending lineaments with ENE-trending lineaments, and (b) these intersections exhibit a major ENE–WSW trend. Suggestion (a) is proven by spatial relationship investigation (Fig. 11) and suggestion (b) is proven by Fry analysis (Fig. 12). About 68 % of the thermal springs in southern South Africa exist within 20 km of an intersection of NNW- and NW-trending lineaments with ENE-trending lineaments.

The Fry points of the intersections of NNW- and NW-trending lineaments with ENE-trending lineaments seem to be distributed along E–W-trending corridors that are regularly spaced at roughly 100 km intervals (Fig. 12). In addition, the spatial distribution of the intersections of NNW- and NW-trending lineaments with ENE-trending lineaments is clustered according to dispersion and arrangement point distribution analyses (Tables 12, 13). Moreover, the spatial distribution of the intersections of NNW- and NW-trending lineaments with ENE-trending lineaments exhibit two box-count fractal dimensions (Fig. 13), one for scales of <100 km wherein these lineament intersections behave like points (i.e., $FD_b = 0.18$) or are strongly clustered, and one for scales of >100 km wherein these lineament intersection behave like lines (i.e., $FD_b = 1.214$). The thermal springs in southern South Africa cluster (i.e., behave like points) within an average of 20 km from an intersection of NNW- and NW-trending lineaments with ENE-trending lineaments, and most of these clusters of thermal springs follow linear trends (i.e., behave like lines) similar to those of ENE–WSW-trending lineaments.

In eastern South Africa, thermal springs have strong positive spatial relationships with ENE- and WNW-trending lineaments (Fig. 10b, h) but exhibit minor ENE–WSW trend in their Fry plot (Fig. 7, Table 7), and they have negative or independent spatial relationships with either NNW- or NW-trending lineaments (Fig. 10f, g) but exhibit major to minor NNW–SSE trends in their Fry plot (Fig. 7, Table 7). These suggest that (a) thermal springs in eastern South Africa have positive spatial relationship with intersections between ENE- and WNW-trending lineaments, and (b) these lineament intersections follow NNW–SSE trends. These suggest that (a) thermal springs in eastern South Africa have positive spatial relationship with intersections of ENE- and WNW-trending lineaments, and (b) these intersections exhibit minor or local-scale ENE–WSW trends. Suggestion (a) is proven by spatial relationship investigation (Fig. 14) and suggestion (b) is proven by Fry analysis (Fig. 15). About 86 % of the thermal springs in eastern South Africa exist within 50 km of an intersection of ENE- and WNW-trending lineaments.

The Fry points of the intersections of ENE- and WNW-trending lineaments seem to be distributed along ENE–WSW-trending corridors that are regularly spaced at roughly 130 km intervals (Fig. 15). In addition, the spatial distribution of the intersections of ENE- and WNW-trending lineaments is largely clustered according to dispersion and arrangement point distribution analyses and partly regular according to arrangement point distribution analysis (Tables 14, 15). Moreover, the spatial distribution of the intersections of NNW- and NW-trending lineaments with ENE-trending lineaments exhibit two box-count fractal dimensions (Fig. 16), one for scales of <50 km wherein these lineament intersections behave like points (i.e., $FD_b = 0.028$) or are strongly clustered, and one for scales of >50 km wherein these lineament intersection behave like lines (i.e., $FD_b = 0.83$). The thermal springs in eastern South Africa cluster (i.e., behave like points) within an average of 50 km from an intersection of ENE- and WNW-trending lineaments, and most of these clusters of thermal springs follow linear trends (i.e.,

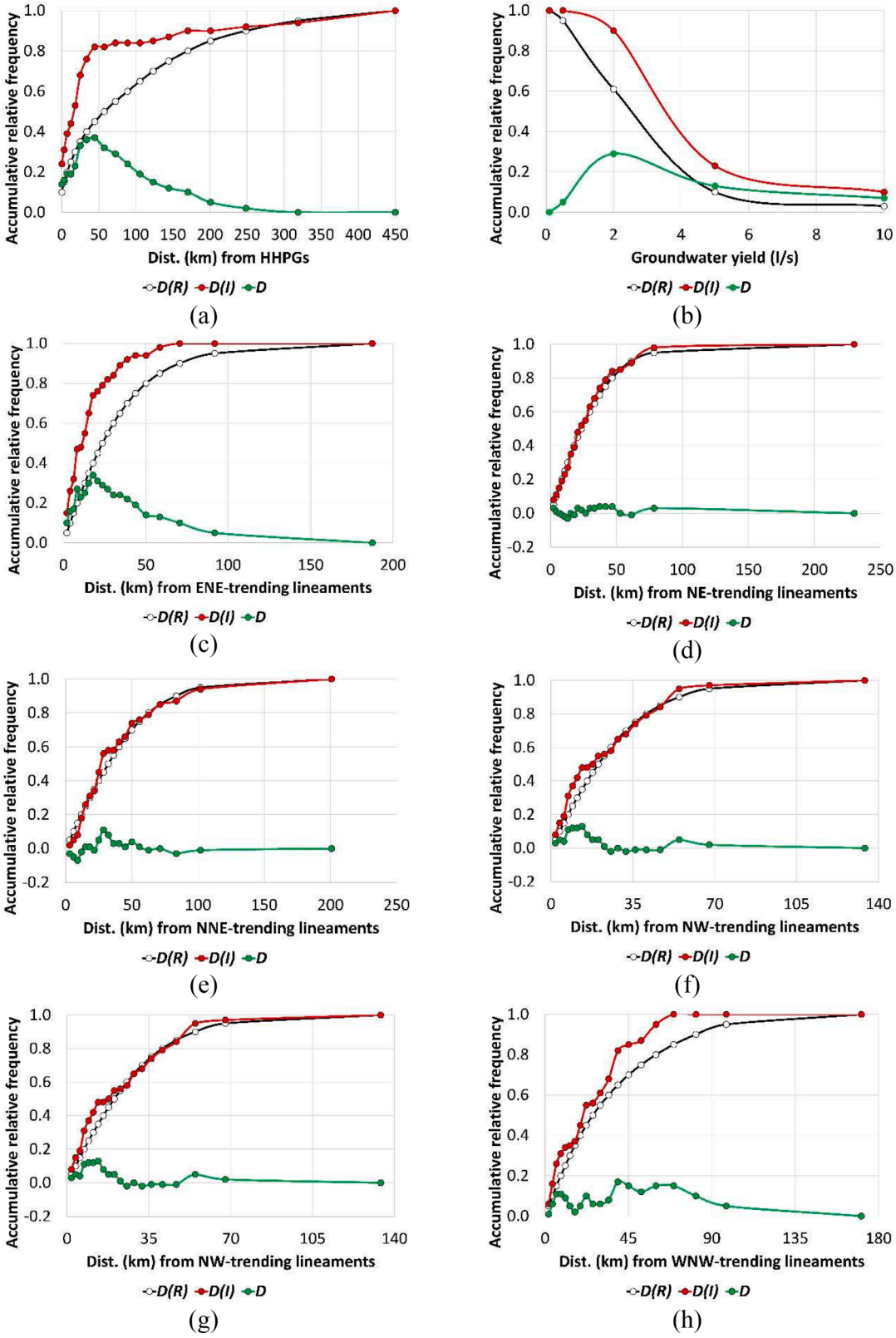

Fig. 8. Whole of South Africa: spatial relationships of thermal springs with (a) high-heat-producing granitoids (HHPGs), (b) groundwater yield, (c) ENE-trending lineaments, (d) NE-trending lineaments, (e) NNE-trending lineaments, (f) NNW-trending lineaments, (f) NW-trending lineaments, and (h) WNW-trending lineaments. See Section 3.2 for explanations of $D(I)$, $D(R)$ and D. The slopes of the $D(I)$ and $D(R)$ curves in (b) differ from those in the other graphs because the proximity analyses depicted in all graphs except those in (b) followed an increasing approach (i.e., from small to large distances from lineaments, as thermal springs are expected to exist close to but not far from faults/fractures) whereas the groundwater analysis followed a decreasing approach (i.e., from high to low groundwater yield, as thermal springs are expected to exist where groundwater is abundant but not scarce). (For interpretation of the references to colour in this figure legend, the reader is referred to the web version of this article).

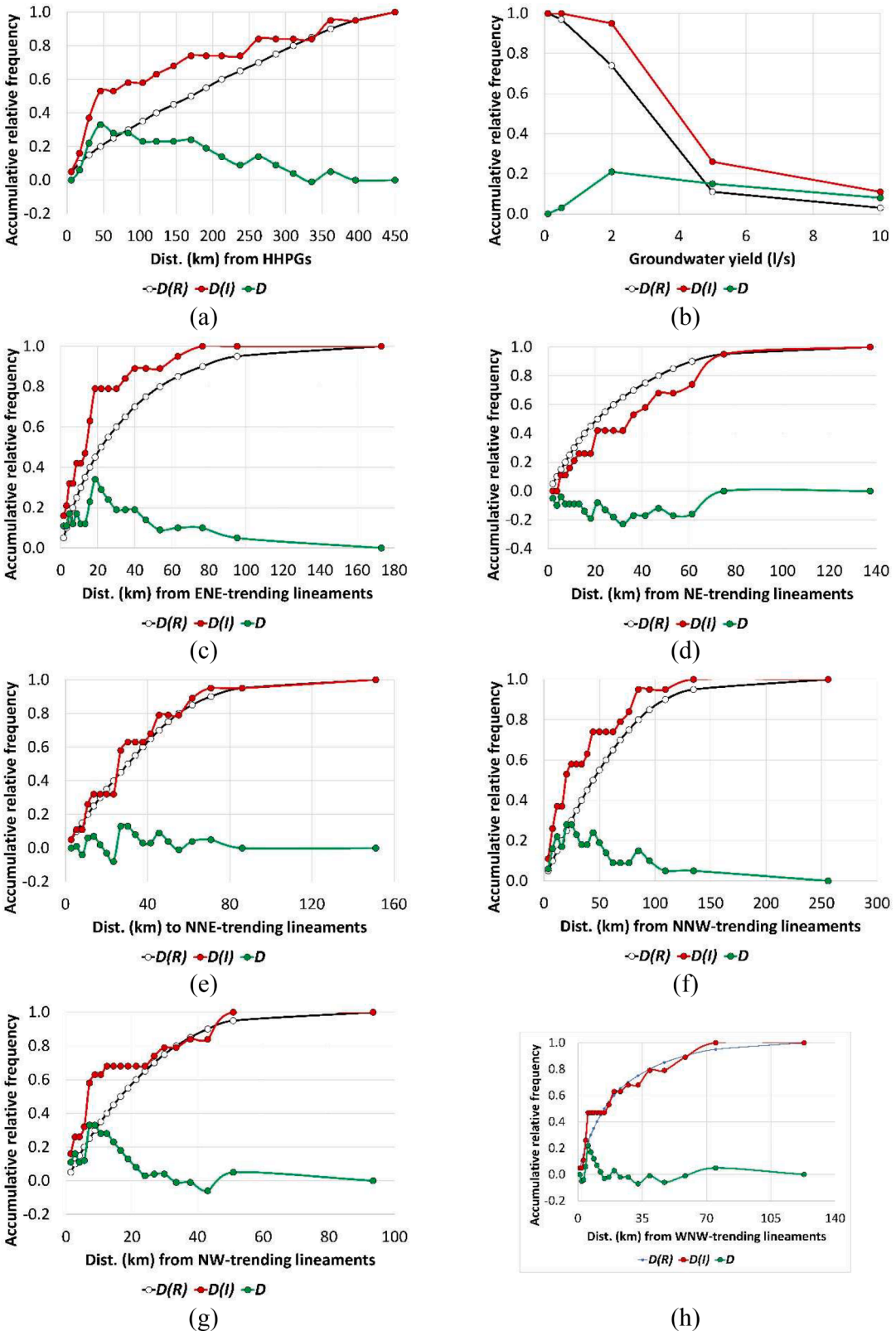

Fig. 9. Southern South Africa: spatial relationships of thermal springs with (a) high-heat-producing granitoids (HHPGs), (b) groundwater yield, (c) ENE-trending lineaments, (d) NE-trending lineaments, (e) NNE-trending lineaments, (f) NNW-trending lineaments, (f) NW-trending lineaments, and (h) WNW-trending lineaments. See Section 3.2 for explanations of $D(I)$, $D(R)$ and D. The slopes of the $D(I)$ and $D(R)$ curves in (b) differ from those in the other graphs because the proximity analyses depicted in all graphs except those in (b) followed an increasing approach (i.e., from small to large distances from lineaments, as thermal springs are expected to exist close to but not far from faults/fractures) whereas the groundwater analysis followed a decreasing approach (i.e., from high to low groundwater yield, as thermal springs are expected to exist where groundwater is abundant but not scarce). (For interpretation of the references to colour in this figure legend, the reader is referred to the web version of this article).

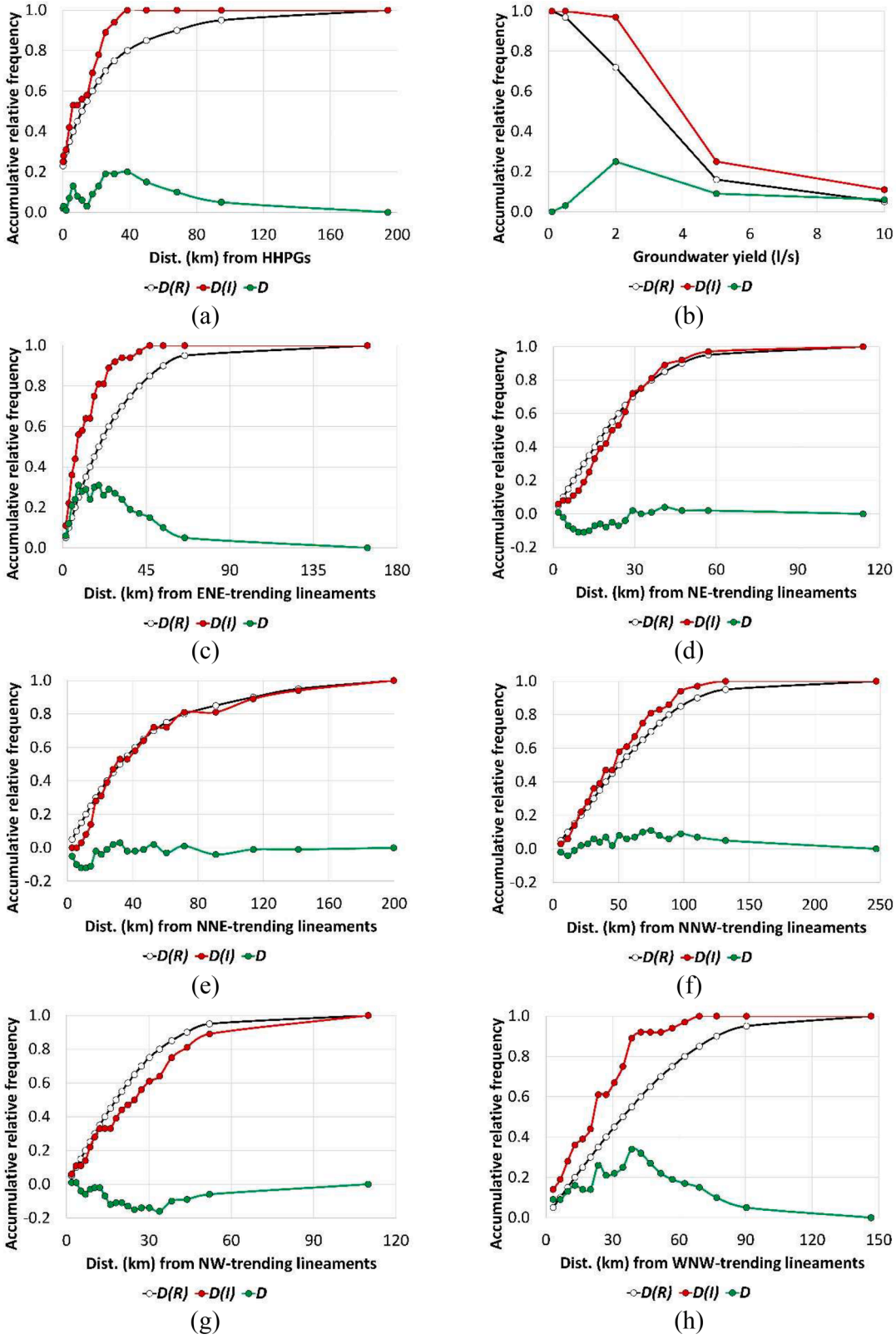

Fig. 10. Eastern South Africa: spatial relationships of thermal springs with (a) high-heat-producing granitoids (HHPGs), (b) groundwater yield, (c) ENE-trending lineaments, (d) NE-trending lineaments, (e) NNE-trending lineaments, (f) NNW-trending lineaments, (f) NW-trending lineaments, and (h) WNW-trending lineaments. See Section 3.2 for explanations of $D(I)$, $D(R)$ and D. The slopes of the $D(I)$ and $D(R)$ curves in (b) differ from those in the other graphs because the proximity analyses depicted in all graphs except those in (b) followed an increasing approach (i.e., from small to large distances from lineaments, as thermal springs are expected to exist close to but not far from faults/fractures) whereas the groundwater analysis followed a decreasing approach (i.e., from high to low groundwater yield, as thermal springs are expected to exist where groundwater is abundant but not scarce). (For interpretation of the references to colour in this figure legend, the reader is referred to the web version of this article).

Table 8
Details of thermal springs' positive spatial relationships with HHPGs in South Africa.

HHPGs in:	Distance (*d*, km) of optimum positive spatial relationship	*D*(*I*) at *d*	*D*(*R*) at *d*	*D*(*I*): *D*(*R*) at *d* (relative strength of spatial relationship)
Whole of South Africa	45	0.82	0.45	1.82
Southern South Africa	46	0.53	0.20	2.65
Eastern South Africa	39	1.00	0.80	1.25

Table 9
Details of thermal springs' positive spatial relationships with groundwater yield in South Africa.

Groundwater yield in:	Groundwater yield (*g*, l/s) of optimum positive spatial relationship	*D*(*I*) at *g*	*D*(*R*) at *g*	*D*(*I*): *D*(*R*) at *g* (relative strength of spatial relationship)
Whole of South Africa	2	0.90	0.61	1.48
Southern South Africa	2	0.95	0.74	1.28
Eastern South Africa	2	0.97	0.72	1.35

Table 10
Details of thermal springs' positive spatial relationships with ENE-trending lineaments in South Africa.

ENE-trending lineaments in:	Distance (*d*, km) from ENE-trending lineaments of optimum positive spatial relationship	*D*(*I*) at *d*	*D*(*R*) at *d*	*D*(*I*): *D*(*R*) at *d* (relative strength of spatial relationship)
Whole of South Africa	18	0.74	0.40	1.85
Southern South Africa	19	0.79	0.45	1.76
Eastern South Africa	19	0.81	0.50	1.62

Table 11
Details of thermal springs' positive spatial relationships with WNW-trending lineaments in South Africa.

ENE-trending lineaments in:	Distance (*d*, km) from WNW-trending lineaments of optimum positive spatial relationship	*D*(*I*) at *d*	*D*(*R*) at *d*	*D*(*I*): *D*(*R*) at *d* (relative strength of spatial relationship)
Whole of South Africa	39	0.82	0.65	1.26
Eastern South Africa	39	0.89	0.60	1.48

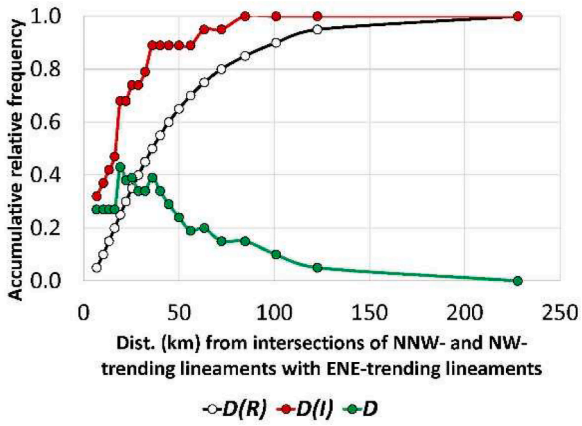

Fig. 11. Southern South Africa: spatial relationship of thermal springs with intersections of NNW- and NW-trending lineaments with ENE-trending lineaments. See Section 3.2 for explanations of *D*(*I*), *D*(*R*) and *D*. (For interpretation of the references to colour in this figure legend, the reader is referred to the web version of this article).

behave like lines) similar to those of ENE–WSW-trending lineaments whereas some of these clusters follow NNW–SSE linear trends.

5. Discussion

5.1. Interpretation of the results

The thermal springs' spatial distribution in South Africa is, based on the point distribution analyses of their dispersion and arrangement, not random but largely clustered and partly regular. Thus, it can be inferred that certain geological features largely controlled the 'focusing' (for largely clustered distribution) and partly controlled the 'spreading' (for partly regular distribution) of thermal waters in the subsurface to the present locations of the thermal springs on the surface. As the averages of observed first- to sixth-order neighbor distances in the dispersion of thermal springs in eastern South Africa were smaller than those in southern South Africa, it can be inferred further that the degree of clustering of thermal springs is stronger in the former region than in the latter region. These inferences were investigated further by fractal and Fry analyses.

The fractal analyses upheld the findings of the point distribution analysis that the degree of clustering of thermal springs in eastern South Africa is stronger than that in southern South Africa. The fractal analyses also upheld the clustered distribution of the thermal springs indicated by the point distribution analysis. The existence of linear trends in the thermal springs' spatial distribution in South Africa, as implied by the fractal analyses, was confirmed by Fry analyses. For the whole of South Africa, the trends for all Fry point pairs can be attributed to regional-scale geological controls, while the trends for only Fry point pairs within minimum distance with the highest probability of finding at least one Fry point next to another Fry point can be ascribed to district-scale geological factors. For eastern and southern South Africa, the trends for all Fry point pairs can be attributed to district-scale geological factors, while the trends for only Fry point pairs within minimum distance with the highest probability of finding at least one Fry point next to another Fry point can be ascribed to local-scale geological factors.

In the whole of South Africa, the interesting trend is NE–SW because it is a major regional-scale trend as well as a minor district-scale trend (Table 7). In southern South Africa, the major ENE–WSW trend, at both district- and local-scales, is interesting (Table 7). In eastern South Africa, there are two interesting trends (Table 7): (1) NNW–SSE, a major district-scale trend and a minor local-scale trend; (2) NE–SW, a minor district-scale trend and a major local-scale trend. These trends are interesting because these are likely the trends of linear geological

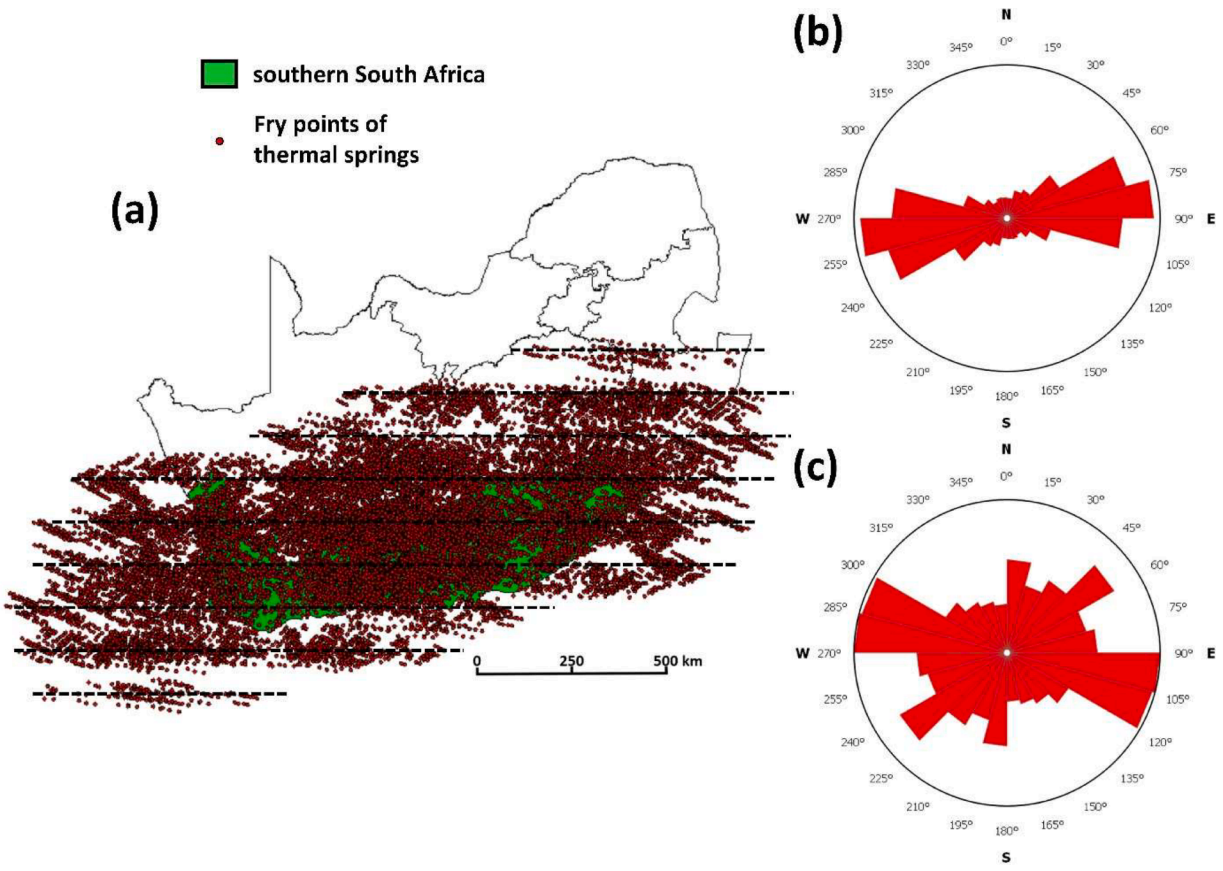

Fig. 12. Spatial distribution of intersections of ENE-trending lineaments with NNW- and NW-trending lineaments in southern South Africa: (a) Fry plot; (b) rose diagram of trends among all Fry point pairs in (a); (c) rose diagram of trends among Fry point pairs within 90 km of each other (i.e., the minimum distance from any lineament intersection within which there is maximum probability that at least one lineament intersection exists next to it). Parallel E–W-trending dashed lines are rough axes of imaginary corridors of Fry points (see Section 4.2.3 for discussion). (For interpretation of the references to colour in this figure legend, the reader is referred to the web version of this article).

Table 12
Results of dispersion analysis of the spatial distribution of intersections of ENE-trending lineaments with NNW- and NW-trending lineaments in southern South Africa.

Order	Averages of neighbor distances (km)	
	Observed	Expected in CSR
1	0.15	0.26
2	0.23	0.39
3	0.30	0.49
4	0.35	0.58
5	0.42	0.65
6	0.47	0.71

Table 13
Results of arrangement analysis of the spatial distribution of intersections of ENE-trending lineaments with NNW- and NW-trending lineaments in southern South Africa.

Order	Number of RCNPs	
	Observed	Expected in CSR
1	98	90.12
2	48	47.72
3	36	35.25
4	36	29.22
5	30	25.52
6	18	22.94

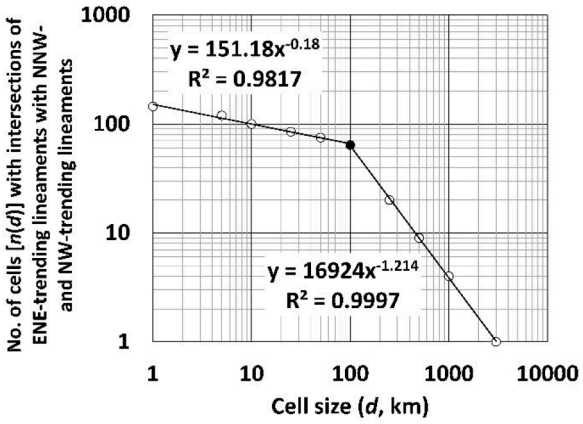

Fig. 13. Log–log plot (white and black dots) defining the following relation of n (d) vs. d for the spatial distribution of intersections of ENE-trending lineaments with NNW- and NW-trending lineaments in southern South Africa.

structures that controlled the thermal springs' occurrence in South Africa. This hypothesis was explored by investigations of spatial relationships of the thermal springs with geological features, the results of which support the findings of the point distribution analysis and fractal analysis that the thermal springs' spatial distributions in South Africa are not random.

The findings of investigations of spatial relationships of thermal springs with ENE-trending geological lineaments support the inference

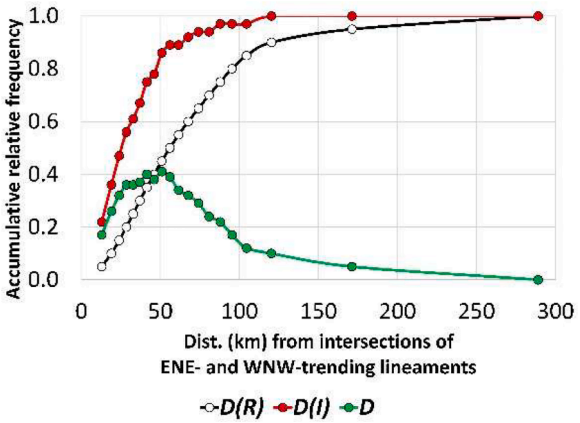

Fig. 14. Eastern South Africa: spatial relationship of thermal springs with intersections of ENE- and WNW-trending lineaments. See Section 3.2 for explanations of *D*(*I*), *D*(*R*) and *D*. (For interpretation of the references to colour in this figure legend, the reader is referred to the web version of this article).

that the major district- and local-scale ENE–WSW trends in the Fry plot of the thermal springs in southern South Africa (Fig. 6, Table 7) are likely due to geological controls rather than to the shape of this district. Overall, the findings of investigations of spatial relationships of thermal springs with ENE-trending geological lineaments suggest that ENE-trending lineaments impose minor ENE–WSW regional- and district-scale trends in the thermal springs' spatial distribution in the whole of South Africa, major ENE–WSW district- and local-scale trends in the thermal springs' spatial distribution in southern South Africa, and minor ENE–WSW local-scale trend in the thermal springs' spatial distribution in eastern South Africa. All these imply that ENE-trending lineaments are important regional- to district-scales, and even local-scale, controls on thermal springs occurrence in South Africa. However, the results of investigations of spatial relationships suggest further that intersections of district-scale NNW- and NW-trending lineaments with regional-scale ENE-trending lineaments control the spatial distribution of thermal springs in southern South Africa, and intersections of regional-scale ENE- and WNW-trending lineaments control the spatial distribution of thermal springs in eastern South Africa.

It is interesting to find that the thermal springs' positive spatial relationships with HHPGs in southern and the whole South Africa are stronger than in eastern South Africa (Table 8). However, the 36 thermal springs in eastern South Africa have an average temperature of 40.6 °C (std. dev. of 8.8 °C) whereas the 20 thermal springs in southern South

Table 14
Results of dispersion analysis of the spatial distribution of intersections of ENE- and WNW-trending lineaments in eastern South Africa.

Order	Averages of neighbor distances (km)	
	Observed	Expected in CSR
1	0.40	0.47
2	0.57	0.70
3	0.73	0.88
4	0.96	1.03
5	1.09	1.15
6	1.24	1.27

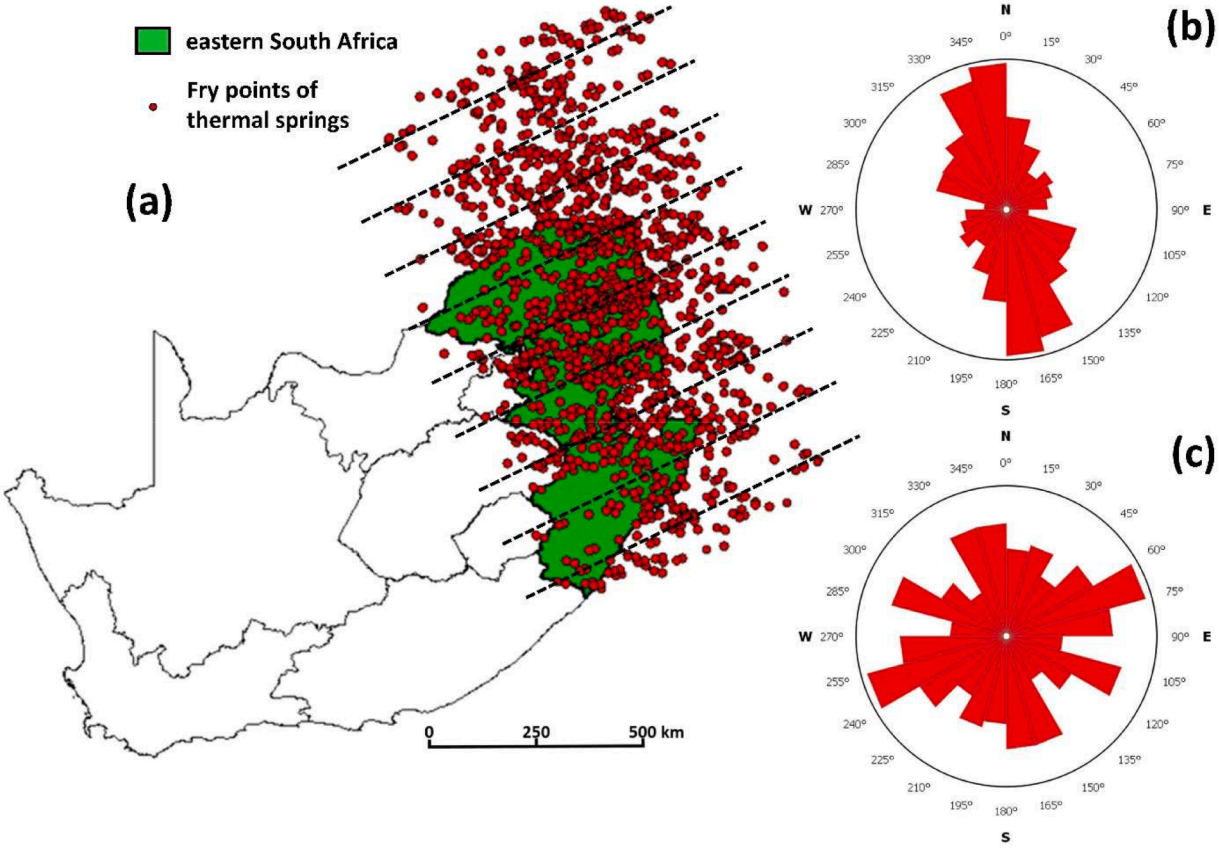

Fig. 15. Spatial distribution of intersections of ENE- and WNW-trending lineaments eastern South Africa: (a) Fry plot; (b) rose diagram of trends among all Fry point pairs in (a); (c) rose diagram of trends among Fry point pairs within 200 km of each other (i.e., the minimum distance from any lineament intersection within which there is maximum probability that at least one lineament intersection exists next to it). Parallel ENE–WNW-trending dashed lines are rough axes of imaginary corridors of Fry points (see Section 4.2.3 for discussion). (For interpretation of the references to colour in this figure legend, the reader is referred to the web version of this article).

Table 15
Results of arrangement analysis of the spatial distribution of intersections ENE- and WNW-trending lineaments in eastern South Africa.

Order	Number of RCNPs	
	Observed	Expected in CSR
1	24	23.62
2	12	12.51
3	10	9.24
4	6	7.66
5	2	6.69
6	8	6.01

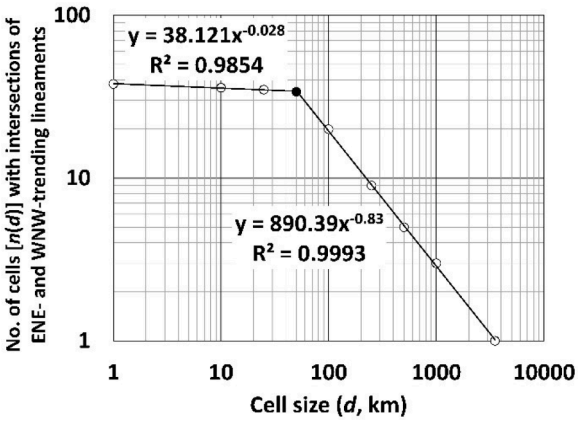

Fig. 16. Log–log plot (white and black dots) defining the following relation of $n(d)$ vs. d for the spatial distribution of intersections of ENE- and WNW-trending lineaments eastern South Africa.

Africa have an average temperature of 38.2 °C (std. dev. of 9.9 °C). Although these average thermal springs' temperatures in eastern and southern Africa are not significantly different from each other (i.e., the ranges of mean ± std. dev. overlap), the thermal springs' relative strengths of positive spatial relationship with the HHPGs suggest that HHPGs are more important controls on thermal spring occurrence in southern South Africa than in eastern South Africa. However, Dhansay et al. (2017) indicated that HHPGs in southern South Africa have relatively greater heat production than those in eastern South Africa. It turns out that the relative strengths of the thermal springs' positive spatial relationship with groundwater yield control the temperatures of these thermal springs, as discussed in the next paragraph.

Considering that the thermal springs' average temperature in southern South Africa is relatively colder than that in eastern South Africa, the thermal springs' relative strengths of positive spatial relationship with groundwater suggest that groundwater yield is a more important control on thermal spring occurrence in eastern South Africa than in southern South Africa. However, inspection of the D curves in Figs. 9a and 10a reveals that, although thermal springs in eastern and southern South Africa have optimum positive spatial relationship with groundwater yield of 2 L/s, thermal springs in southern South Africa have relatively stronger positive spatial relationship with groundwater yield of >2 L/s compared to those in eastern South Africa. This would explain why the thermal springs in southern South Africa are relatively colder than those in eastern South Africa (i.e., more water, lower temperature).

5.2. Conceptual model of thermal springs occurrence

From the preceding interpretation of results of spatial investigations, a conceptual model of regional- to district-scale geological controls on thermal springs occurrence in southern South Africa and another one in eastern South Africa can be made but not in the whole of South Africa. That is because almost all the thermal springs in this country exist in its southern and eastern parts and because the results of spatial investigations in these two different districts are somewhat dissimilar.

In southern South Africa, regional- to district-scale geological controls on thermal springs occurrence involve the presence of or proximity to HHPGs (as heat source control), groundwater yield of ~2 L/s (as water source control) and intersections of ENE-trending lineaments with NNW- and NW-trending lineaments (as pathways control). This deduced pathways control on thermal springs occurrence by intersections of ENE-trending lineaments with NNW- and NW-trending lineaments is not inconsistent with field knowledge that several thermal springs in southern South Africa are linked to generally E–W-trending faults (Diamond and Harris, 2000; Madi et al., 2016). The finding of this study implies that thermal springs in southern South Africa are controlled by generally E–W-trending, or specifically ENE-trending, structures and particularly where these structures are intersected by NNW- and NW-trending structures.

In eastern South Africa, regional- to district-scale geological controls on thermal springs occurrence involve the presence of or proximity to HHPGs (as heat source control), groundwater yield of ~2 L/s (as water source control) and intersections of ENE- and WNW-trending lineaments (as pathways control). Thus, based on available relevant data, regional- to district-scale geological controls on thermal springs occurrence in southern and eastern South Africa differ mainly in pathways control. This main difference in the regional- to district-scale geological controls on thermal springs occurrence in southern and eastern South Africa can be attributed to the striking differences in tectonisms that affected southern and eastern South Africa, as depicted roughly in Fig. 1 and which are discussed extensively in the literature (e.g., Kisters et al., 2002; Kramers et al., 2014; Humbert et al., 2020; Owolabi et al., 2021). Because thermal springs are a surface manifestation of geothermal resources, the respective conceptual models of regional- to district-scale geological controls on thermal springs occurrence in southern and eastern South Africa can now be used to guide predictive modeling and mapping of the prospectivity (or likelihood) of areas where geothermal resources potentially exist within these districts. This will be demonstrated in sequel paper; however, a few examples of predictive geothermal resource prospectivity mapping can be found in the literature (e.g., Kiavarz & Jelokhani-Niaraki, 2017; Yusuf et al., 2021; Lacasse et al., 2022). The conceptual models of regional- to district-scale geological controls on thermal springs occurrence in southern and eastern South Africa presented above can be improved depending on availability of relevant regional- to district-scale geoscience spatial data. For example, data on regional- to district- scale geothermal heat flux (e.g., Rysgaard et al., 2018; Wei et al., 2022) and thermophysical properties of rocks (e.g., Zhu et al., 2023) would be useful in tweaking the above-presented conceptual models of regional- to district-scale geological controls on thermal springs occurrence in southern and eastern South Africa. However, these sorts of data are unavailable in South Africa.

5.3. Remarks on the methods of spatial investigation

Results of point distribution analysis, fractal analysis and Fry analysis complement and supplement each other in the investigation of the spatial distribution of known thermal spring occurrences at particular spatial scales. Investigation at a particular spatial scale is stressed here for it is improper to deduce controls on thermal spring occurrence at, for example, spring-scale baed on regional-scale spatial data. Thus, as regional- to district-scale data were used in this study, they are inappropriate for elucidation of local- to spring-scale geological controls on thermal spring occurrence. However, the subdivision of the whole of South Africa into districts based on administrative provincial boundaries (Fig. 3) allowed us to investigate the thermal springs' spatial distributions by Fry analyses at district- to local-scales, from which inferences of local-scale controls were made even though regional- to district-scale

data were used.

The results of investigations show that point distribution, fractal and Fry analyses yield distinct yet more-or-less coherent details of the thermal springs' spatial distribution, which can be combined into a consistent interpretation. Point distribution analysis is beneficial chiefly for a broad description of the sort of spatial distribution. Box-count fractal analysis is valuable largely for deducing the scales at which particular controls on thermal spring occurrence operate. Fry analysis is advantageous for visualization of which linear geological features are likely controls on thermal spring occurrence. Thus, for an investigation with the same or similar goal(s) as this present one, it is worthwhile to use these methods in combination with each other instead of employing only one of them.

However, investigation of only the spatial distribution of thermal springs is inadequate for conceptual modelling of controls on their occurrence. Investigations of spatial distribution of thermal springs should be upheld by investigations of their spatial relationships with geological features through, for example, distance distribution analysis, as in this study, so that a sound conceptual model of controls on thermal spring occurrence can be drawn. Proximity or buffer analysis in GIS (e.g., Omwenga et al., 2017; Abuzied et al., 2020), which is a generic term for different versions of distance distribution analysis, may also be used to substantiate the investigation of the spatial distribution of thermal springs for conceptual modelling of their geological controls at particular spatial scales. For example, geological boundaries between certain domains are zonal, often defined by a zone width of tens to hundreds of kilometers, which would affect the distribution of thermal springs; however, this could addressed by complementing spatial distribution analysis with proximity or buffer analysis in GIS (Rahmati et al., 2019). In addition, the methods of spatial investigations presented here are dependent on the amount of point data representing locations of thermal springs. Accordingly, investigation of the spatial distribution of the few thermal springs outside eastern and southern South Africa (Fig. 3) by either point pattern analysis of fractal analysis will not yield geologically meaningful results.

5.4. Limitations of the study

Besides the limitation of the methods used being dependent on the amount of point data representing locations of thermal springs, the findings of this study are constrained by the scale and type of data/maps used to explore/explain the geological significance of the spatial distribution of thermal springs and their spatial relationships with certain geological features. The regional-scale datasets used in this study were 2-dimensional, and so 3-dimensional (3D) orientations of structures were not considered in this study. However, consideration of 3D orientations of geological features is appropriate in local-scale investigations but not in regional- to district-scale investigations, as in this present study. That is because 3D regional- to district-scale geological data are typically not only sparse but also sporadically distributed, and that would result in bias towards local areas where 3D local-scale geological data available.

Another limitation of the study is that, as 3D orientations of structures were not taken into consideration in this study, stress fields associated with geological structures were also not considered in this study. One would expect that, depending on the orientation relative to the surrounding stresses, certain structures/zones would be more amenable for the occurrence of thermal springs. This limitation was addressed, however, by using in the spatial investigations different sets of lineaments according to their strikes (see sub-Sections 4.2.2 and 4.2.3). That is because the strike of a geological structure is a function of the surrounding stresses. In addition, the limitation of not using stress data was addressing by investigating the spatial relationship of the thermal springs with intersections of geological lineaments (see sub-Section 4.2.4). That is because high values of shear stress exist at/around fault intersections or fault discontinuities (Segall and Pollard, 1980) and groundwater flow is directly proportional to shear stress (Gudmundsson et al., 2003).

6. Conclusions

This research, like the earlier studied mentioned in the Introduction section, has demonstrated that thermal spring occurrences exhibit a non-random spatial distribution. Whereas the individual earlier studies mentioned in the Introduction section used Fry analysis to investigate the spatial distribution of thermal springs, this study has used point distribution and fractal analyses besides Fry analysis to unravel the thermal springs' regional- to district-scale spatial distribution in South Africa. These three different methods for spatial investigation of a distribution of point bodies, such as thermal springs on regional to district scales, complement and supplement each other. According to the outcomes of using these three spatial investigation methods, the known thermal spring occurrences in South Africa exhibit marked distributions at district scales (i.e., $\leq$100 km search radii from thermal spring occurrence) and at regional scales (i.e., $>$100 km search radii from each thermal spring occurrence). At district-scales, the known thermal springs in southern South Africa exhibit a largely clustered and partly regular spatial distribution of mostly ENE-trending fractal point objects associated with NNW- and NW-trending lineaments (Figs. 5, 9) whereas the known thermal springs in eastern South Africa exhibit a largely clustered and partly regular spatial distribution of mostly NNW-trending fractal point objects associated with ENE- and -WNW-trending lineaments (Figs. 7, 10). At regional scales, clusters of known thermal springs in South Africa exhibit a regular spatial distribution of fractal linear objects with major NE–SW trend and minor WNW–ESE trend (Fig. 5).

The results of spatial investigations indicate that, on a regional-scale, thermal spring occurrences in southern South Africa are controlled by intersections of ENE-trending lineaments with NNW- and NW-trending lineaments whereas thermal spring occurrences in eastern South Africa are controlled by intersections of ENE- and WNW-trending lineaments. These structural lineament intersections serve as pathways control for heated groundwater to migrate from the subsurface to the surface. The difference in pathways control on migration of heated groundwater for thermal springs occurrence in southern and eastern South Africa, as captured by the spatial investigations, is supported by knowledge that these different regions are defined by different geological/tectonic domains. Besides this spatial information on pathways control, the results of spatial investigations revealed that regional- to district-scale geological controls on thermal springs occurrence in South Africa involve the presence of or proximity to HHPGs (as heat source control) and groundwater yield of $\sim$2 L/s (as water source control).

The use of the methods discussed in this paper for spatial distribution and spatial relationship investigations helps in conceptual modeling of geological factors of thermal springs occurrence at certain spatial scales. A conceptual model of geological factors of thermal springs occurrence at certain spatial scales will be useful in regional- to district-scale predictive modeling and mapping of the prospectivity (or likelihood) of areas where geothermal resources potentially exist in South Africa. However, the proposed conceptual model of regional- to district-scale geological factors of thermal springs occurrence in South Africa must be amended when new or additional appropriate geoscience spatial data become available.

CRediT authorship contribution statement

Emmanuel John M. Carranza: Conceptualization, Data curation, Formal analysis, Funding acquisition, Investigation, Methodology, Project administration, Resources, Software, Supervision, Validation, Visualization, Writing – original draft. **Reinnie Ntokozo Maseko:** Formal analysis, Investigation, Validation, Visualization.

Declaration of Competing Interest

The authors declare that they have no known competing financial interests or personal relationships that could have appeared to influence the work reported in this paper.

Acknowledgment

The study discussed here was part of a research project funded by the National Research Foundation (NRF) of South Africa (grant no. 118471) under the South Africa / Mozambique / Zambia Trilateral Joint Science and Technology Research Collaboration program. Part of the study presented here was part of the second author's BSc Honours project at the University of KwaZulu-Natal.

References

Abiye, T.A., Tshipala, D., Leketa, K., Villholth, K.G., Ebrahim, G.Y., Magombeyi, M., Butler, M., 2020. Hydrogeological characterization of crystalline aquifer in the Hout River Catchment, Limpopo province, South Africa. Groundw. Sustain. Dev. 11, 100406.

Abuzied, S.M., Kaiser, M.F., Shendi, E.A.H., Abdel-Fattah, M.I, 2020. Multi-criteria decision support for geothermal resources exploration based on remote sensing, GIS and geophysical techniques along the Gulf of Suez coastal area, Egypt. Geothermics 88, 101893.

Barnett, W., Armstrong, R.A., de Wit, M.J., 1997. Stratigraphy of the upper Neoproterozoic Kango and lower Palaeozoic table mountain groups of the cape fold belt revisited. S. Afr. J. Geol. 100 (3), 237–250.

Basantaray, A.K., Mandal, A., 2022. Interpretation of gravity–magnetic anomalies to delineate subsurface configuration beneath east geothermal province along the Mahanadi rift basin: a case study of non-volcanic hot springs. Geotherm. Energy 10 (1), 1–27.

Bell, J.W., Ramelli, A.R., 2009. Active fault controls at high-temperature geothermal sites: prospecting for new faults. Geotherm. Resour. Counc. Trans. 33, 425–429.

Berman, M., 1977. Distance distributions associated with Poisson processes of geometric figures. J. Appl. Probab. 14, 195–199.

Berman, M., 1986. Testing for spatial association between a point processes and another stochastic process. Appl. Stat. 35, 54–62.

Boots, B.N., Getis, A., 1988. Point pattern analysis. Sage University Scientific Geography Series No. 8. Sage Publications, Beverly Hills, p. 93.

Botha, B.J.V., Grobler, N.J., Burger, A., 1979. New U-Pb age-measurements on the Koras Group, Cape Province and its significance as a time-reference horizon in eastern Namaqualand. S. Afr. J. Geol. 82 (1), 1–5.

Browning, C., Macey, P.H., 2015. Lithostratigraphy of the george pluton units (Cape granite suite), South Africa. S. Afr. J. Geol. 118 (3), 323–330.

Carlson, C.A., 1991. Spatial distribution of ore deposits. Geology 19, 111–114.

Carranza, E.J.M., 2002. Geologically-constrained mineral potential mapping (Examples from the Philippines). Ph.D. Thesis, Delft University of Technology, The Netherlands. ITC Publication No. 86 (ISBN 90-6164-203-5), 480 pp. https://webapps.itc.utwente.nl/librarywww/papers/phd_2002/carranza.pdf.

Carranza, E.J.M., 2008. Geochemical Anomaly and Mineral Prospectivity Mapping in GIS. Handbook of Exploration and Environmental Geochemistry, 11. Elsevier, Amsterdam, p. 351.

Carranza, E.J.M., 2009. Controls on mineral deposit occurrence inferred from analysis of their spatial pattern and spatial association with geological features. Ore Geol. Rev. 35 (3-4), 383–400.

Carranza, E.J.M., Wibowo, H., Barritt, S.D., Sumintadireja, P., 2008. Spatial data analysis and integration for regional-scale geothermal potential mapping, West Java, Indonesia. Geothermics 37 (3), 267–299.

Catuneanu, O., Wopfner, H., Eriksson, P.G., Cairncross, B., Rubidge, B.S., Smith, R.M.H., Hancox, P.J., 2005. The Karoo basins of south-central Africa. J. Afr. Earth Sci. 43 (1-3), 211–253.

Cheng, Q., Agterberg, F.P., Bonham-Carter, G.F., 1996. Fractal pattern integration for mineral potential estimation. Nonrenew. Resour. 5, 117–130.

Clifford, T.N., Gronow, J., Rex, D.C., Burger, A.J., 1975. Geochronological and petrogenetic studies of high-grade metamorphic rocks and intrusives in Namaqualand, South Africa. J. Petrol. 16 (1), 154–188.

Compston, W., Kröner, A., 1988. Multiple zircon growth within early Archaean tonalitic gneiss from the Ancient Gneiss Complex, Swaziland. Earth Planet. Sci. Lett. 87 (1-2), 13–28.

Cox, T.F., 1981. Reflexive nearest neighbours. Biometrics 37, 367–369.

Dhansay, T., Musekiwa, C., Ntholi, T., Chevallier, L., Cole, D., De Wit, M.J., 2017. South Africa's geothermal energy hotspots inferred from subsurface temperature and geology. S. Afr. J. Sci. 113 (11-12), 1–7.

Diamond, R.E., Harris, C., 2000. Oxygen and hydrogen isotope geochemistry of thermal springs of the Western Cape, South Africa: recharge at high altitude? J. Afr. Earth Sci. 31 (3-4), 467–481.

Du Plessis, C.P., Walraven, F., 1990. The tectonic setting of the Bushveld complex in Southern Africa, Part 1. Structural deformation and distribution. Tectonophysics 179 (3-4), 305–319.

Du Toit, A., 1954. The Geology of South Africa, 3d ed., rev. and enl ed. Oliver and Boyd, Edinburgh.

Eriksson, P.G., Hattingh, P.J., Altermann, W., 1995. An overview of the geology of the Transvaal sequence and Bushveld complex, South Africa. Miner. Depos. 30 (2), 98–111.

Ford, A., Blenkinsop, T.G., 2008. Combining fractal analysis of mineral deposit clustering with weights of evidence to evaluate patterns of mineralization: application to copper deposits of the Mount Isa Inlier, NW Queensland, Australia. Ore Geol. Rev. 33, 435–450.

Fripp, R.E.P., Van Nierop, D.A., Callow, M.J., Lilly, P.A., Du Plessis, L.U., 1980. Deformation in part of the Archaean Kaapvaal craton, South Africa. Precambrian Res. 13 (2-3), 241–251.

Fry, N., 1979. Random point distributions and strain measurement in rocks. Tectonophysics 60, 89–105.

Ghosh, S., Carranza, E.J.M., 2010. Spatial analysis of mutual fault/fracture and slope controls on rocksliding in Darjeeling Himalaya, India. Geomorphology 122 (1-2), 1–24.

Gorum, T., Carranza, E.J.M., 2015. Control of style-of-faulting on spatial pattern of earthquake-triggered landslides. Int. J. Environ. Sci. Technol. 12, 3189–3212.

Gravelet-Blondin, K. R. (2013). A geological and hydrogeological study of the Shu Shu thermal springs, KwaZulu-Natal. Masters thesis, University of KwaZulu-Natal, 170 p. (https://ukzn-dspace.ukzn.ac.za/handle/10413/11177).

Gudmundsson, A., Gjesdal, O., Brenner, S.L., Fjeldskaar, I., 2003. Effects of linking up of discontinuities on fracture growth and groundwater transport. Hydrol. J. 11, 84–99.

Humbert, F., Agangi, A., Massuyeau, M., Elburg, M.A., Belyanin, G., Smith, A.J., Wabo, H., 2020. Rifting of the Kaapvaal Craton during the early Paleoproterozoic: evidence from magmatism in the western Transvaal subbasin (South Africa). Precambrian Res. 342, 105687.

Jelsma, H.A., De Wit, M.J., Thiart, C., Dirks, P.H., Viola, G., Basson, I.J., Anckar, E., 2004. Preferential distribution along transcontinental corridors of kimberlites and related rocks of Southern Africa. S. Afr. J. Geol. 107 (1-2), 301–324.

Johnson, M. R., 1976. Stratigraphy and sedimentology of the Cape and Karoo sequences in the Eastern Cape Province. PhD thesis, Rhodes University, 351 pp.

Johnson, M.R., Van Vuuren, C.J., Hegenberger, W.F., Key, R., Show, U., 1996. Stratigraphy of the Karoo Supergroup in southern Africa: an overview. J. Afr. Earth Sci. 23 (1), 3–15.

Johnson, M.R., Anhauesser, C.R., Thomas, R.J. (Eds.), 2006. The Geology of South Africa. Geological Society of South Africa, Johannesburg/Council for Geoscience, Pretoria, p. 691.

Kent, L.E., 1949. The thermal waters of the Union of South Africa and South West Africa. S. Afr. J. Geol. 52 (1), 231–264.

Kiavarz, M., Jelokhani-Niaraki, M., 2017. Geothermal prospectivity mapping using GIS-based ordered weighted averaging approach: a case study in Japan's Akita and Iwate provinces. Geothermics 70, 295–304.

Kisters, A.F., Belcher, R.W., Scheepers, R., Rozendaal, A., Jordaan, L.S., Armstrong, R.A., 2002. Timing and kinematics of the Colenso fault: the early Paleozoic shift from collisional to extensional tectonics in the Pan-African Saldania Belt, South Africa. S. Afr. J. Geol. 105 (3), 257–270.

Kramers, J.D., Henzen, M., Steidle, L., 2014. Greenstone belts at the northernmost edge of the Kaapvaal Craton: timing of tectonic events and a possible crustal fluid source. Precambrian Res. 253, 96–113.

Lacasse, C.M., Prado, E.M.G., Guimarães, S.N.P., de Souza Filho, O.A., Vieira, F.P., 2022. Integrated assessment and prospectivity mapping of geothermal resources for EGS in Brazil. Geothermics 100, 102321.

Madi, K., Nyabeze, P., Gwavava, O., Sekiba, M., Zhao, B., 2014. Uranium, thorium and potassium occurrences in the vicinity of hot springs in the northern neotectonic belt in the Eastern Cape Province, South Africa. J. Radioanal. Nucl. Chem. 301, 351–363.

Madi, K., Nyabeze, P.K., Gwavava, O., Sekiba, M., Zhao, B., 2016. Magnetic and electromagnetic signatures around Polile Tshisa hot spring in the northern neotectonic belt in the eastern Cape Province, South Africa. Acta Geophys. 64, 943–962.

Mandelbrot, B.B., 1982. The Fractal Geometry of Nature. Freeman, New York, p. 460.

Mandelbrot, B.B., 1985. Self-affine fractals and fractal dimension. Phys. Scr. 32, 257–260.

McCarthy, T. S., Johnson, M. R., Anhauesser, C. R., & Thomas, R. J., 2006. The witwatersrand supergroup. The Geology of South Africa, 155-186.

McCarthy, T.S., Rubidge, B., 2005. The Story of Earth & Life. A Southern African Perspective on a 4.6-Billion-Year Journey. Struik Publishers, Cape Town, p. 334.

McCourt, S., Armstrong, R.A., 1998. SHRIMP U-Pb zircon geochronology of granites from the Central Zone, Limpopo Belt, Southern Africa: implications for the age of the Limpopo Orogeny. S. Afr. J. Geol. 101 (4), 329–338.

Moghaddam, M.K., Noorollahi, Y., Samadzadegan, F., Sharifi, M.A., Itoi, R., 2013. Spatial data analysis for exploration of regional scale geothermal resources. J. Volcanol. Geotherm. Res. 266, 69–83.

Moghaddam, M.K., Samadzadegan, F., Noorollahi, Y., Sharifi, M.A., Itoi, R., 2014. Spatial analysis and multi-criteria decision making for regional-scale geothermal favorability map. Geothermics 50, 189–201.

Nowicki, T.E., Frimmel, H.E., Waters, D.J., 1995. The occurrence of osumilite in pelitic granulites of the Namaqualand Metamorphic Complex, South Africa. S. Afr. J. Geol. 98 (2), 191–201.

Omwenga, B., Katana, C., Rutto, E., Musyoka, C., 2017. Integration of geological modelling approach and GIS in exploration and well targeting in the olkaria geothermal area. Trans. Geotherm. Resour. Counc. 41, 1554–1561.

Owolabi, S.T., Madi, K., Kalumba, A.M., Baiyegunhi, C., 2021. A geomagnetic analysis for lineament detection and lithologic characterization impacting groundwater

prospecting; a case study of Buffalo catchment, Eastern Cape, South Africa. Groundw. Sustain. Dev. 12, 100531.
Rahmati, A.R., Moradzadeh, A., Pahlavani, P., Rahmani, M.R., 2019. Using index and cumulative overlay analyses to determine geothermal potential targets in damavand region. The international archives of the photogrammetry. Remote Sens. Spat. Inf. Sci. 42, 867–873.
Robb, L.J., Meyer, F.M., 1995. The Witwatersrand Basin, South Africa: geological framework and mineralization processes. Ore Geol. Rev. 10 (2), 67–94.
Rysgaard, S., Bendtsen, J., Mortensen, J., Sejr, M.K., 2018. High geothermal heat flux in close proximity to the Northeast Greenland Ice Stream. Sci. Rep. 8 (1), 1–8.
Sadigh, S., Mirmohammadi, M., Asghari, O., Porwal, A., 2022. Spatial distribution of porphyry copper deposits in Kerman Belt, Iran. Ore Geol. Rev. 153, 105251.
Sang, X., Xue, L., Liu, J., Zhan, L., 2017. A novel workflow for geothermal prospectively mapping weights-of-evidence in Liaoning Province, Northeast China. Energies 10 (7), 1069.
Schmitz, M.D., Bowring, S.A., de Wit, M.J., Gartz, V., 2004. Subduction and terrane collision stabilize the western Kaapvaal craton tectosphere 2.9 billion years ago. Earth Planet. Sci. Lett. 222 (2), 363–376.
Segall, P., Pollard, D.D., 1980. Mechanics of discontinuous faults. J. Geophys. Res. Solid Earth 85 (B8), 4337–4350.
Siégel, C., Schrank, C.E., Bryan, S.E., Beardsmore, G.R., Purdy, D.J., 2014. Heat-producing crust regulation of subsurface temperatures: A stochastic model re-evaluation of the geothermal potential in southwestern Queensland, Australia. Geothermics 51, 182–200.
Singh, H.K., Sinha, S.K., Alam, M.A., Chandrasekharam, D., 2020. Tracing the evolution of thermal springs in the Hazaribagh area of Eastern Peninsular India through hydrogeochemical and isotopic analyses. Geothermics 85, 101817.
Taillefer, A., Guillou-Frottier, L., Soliva, R., Magri, F., Lopez, S., Courrioux, G., Millot, R., Ladouche, B., Le Goff, E., 2018. Topographic and faults control of hydrothermal circulation along dormant faults in an orogen. Geochem. Geophys. Geosyst. 19 (12), 4972–4995.
Thomas, R.J., 1989. A tale of two tectonic terranes. S. Afr. J. Geol. 92 (4), 306–321.
Thomas, R.J., Marshall, C.G.A., Watkeys, M.K., Fitch, F.J., Miller, J.A., 1992. K-Ar and 40Ar/39Ar dating of the Natal Group, Southeast Africa: a post Pan-African molasse? J. Afr. Earth Sci. 15 (3-4), 453–471 (and the Middle East).
Tshibalo, A.E., Dhansay, T., Nyabeze, P., Chevallier, L., Musekiwa, C., Olivier, J., 2015. Evaluation of the geothermal energy potential for South Africa. In: Daniilidis, A., Herber, R. (Eds.), Proceedings of the World Geothermal Congress 2015, Melbourne, Australia, 19-25 April 2015, p. 9 p.
Van Reenen, D.D., Roering, C., Ashwal, L.D., De Wit, M.J., 1992. Regional geological setting of the Limpopo Belt. Precambrian Res. 55 (1-4), 1–5.
Wei, S.C., Liu, F., Zhang, W., Wang, G.L., Yuan, R.X., Liao, Y.Z., Yan, X.X., 2022. Research on the characteristics and influencing factors of terrestrial heat flow in Guizhou Province. J. Groundw. Sci. Eng. 10 (2), 166–183.
Weiberg, R.F., Hodkiewicz, P.F., Groves, D.I., 2004. What controls gold distribution in Archean terranes? Geology 32, 545–548.
Yusuf, A., San, L.H., Abir, I.A., 2021. A Preliminary geothermal prospectivity mapping based on integrated GIS, remote-sensing, and geophysical techniques around Northeastern Nigeria. Sustainability 13 (15), 8525.
Zehner, R.E., Coolbaugh, M.F., Shevenell, L., 2006. Regional groundwater geochemical trends in the Great Basin: implications for geothermal exploration. Geotherm. Resour. Counc. Trans. 30, 117–124.
Zheng, D., Ni, C., Zhang, S., Chen, Z., Zhong, J., Zhu, J., Yan, Y., 2020. Significance of the spatial point pattern and Fry analysis in mineral exploration. Arabian J. Geosci. 13, 1–11.
Zhu, X., Gao, Z., Chen, T., Wang, W., Lu, C., Zhang, Q., 2023. Study on the thermophysical properties and influencing factors of regional surface shallow rock and soil in China. Front. Earth Sci. 10, 864548.